UNIVERSIDADE FEDERAL DE MINAS GERAIS
Curso de Pós-Graduação em Engenharia Metalúrgica e de Minas

Tese de Doutorado

"Fixação da espécie trivalente de arsênio em oxi-hidróxidos de ferro e de alumínio: avaliação de mecanismos moleculares e suas implicações na mobilidade do arsênio no meio ambiente"

Autora: Graziele Duarte
Orientadora: Professora Virgínia S. T. Ciminelli
Co-orientador: Professor Kwadwo Osseo-Asare

Junho de 2010

UNIVERSIDADE FEDERAL DE MINAS GERAIS
Curso de Pós-Graduação em Engenharia Metalúrgica e de Minas

Graziele Duarte

"Fixação da espécie trivalente de arsênio em oxi-hidróxidos de ferro e de alumínio: avaliação de mecanismos moleculares e suas implicações na mobilidade do arsênio no meio ambiente"

"Fixation of As(III) species on iron and aluminum oxy-hydroxides: evaluation of molecular mechanisms and their implications on arsenic mobility in the environment"

Tese de Doutorado apresentada ao Curso de Pós-Graduação em Engenharia Metalúrgica e de Minas da Universidade Federal de Minas Gerais

Área de Concentração: Tecnologia Mineral
Orientadora: Professora Virgínia S. T. Ciminelli
Co-orientador: Professor Kwadwo Osseo-Asare- Penn State Unniversity

Belo Horizonte
Escola de Engenharia da UFMG
2010

Dedico esta tese ao meu paizão,Tarcízio
e à minha mãezinha, Maria de Lourdes.

AGRADECIMENTOS

"É bom olhar pra trás e admirar a vida que soubemos fazer..."

Esse trecho de uma música que gosto muito resume bem o que sinto nesse momento. Quando olho para trás e recordo cada etapa dessa jornada, me vem uma imensurável satisfação de constatar que tudo valeu a pena. E não somente por causa do resultado hoje apresentado, que por si só já seria motivo de muito orgulho, mas principalmente pelo caminho percorrido até aqui. Um caminho iluminado pela presença de pessoas muito especiais, as quais eu agradeço do fundo do meu coração.

Em primeiro lugar agradeço aos meus pais Tarcízio e Maria de Lourdes, pelo exemplo e apoio incondicional, e por construírem com muito amor e sabedoria uma família linda, da qual eu me orgulho tanto de fazer parte! Às minhas irmãs Denise, Janete, Patrícia e Aline, agradeço pela presença constante em minha vida, pelo grande amor e amizade que nos une. Aos meus sobrinhos, Larissa, Caio, Alice, Clara, Cecília, João Pedro, Theo e Sara por encherem o coração dessa tia coruja com tantas alegrias! Aos meus cunhados Marcelinho e Paulo, por todo carinho. E ao meu amor, Fabiano - que chegou trazendo a luz que faltava, eu agradeço todo o incentivo, força, compreensão, amizade e amor que me dedica a cada dia. Amo vocês!

Agradeço a todos os meus amigos pelo carinho, pela certeza de poder contar sempre com vocês, pelo ombro e pelos ouvidos a mim emprestados tantas vezes nesses anos! Em especial agradeço à Michelle, Carol, Denise e Cynthia, minhas irmãs de coração!

A todos os colegas do Laboratório de Processamentos aquosos, que foram muitos ao longo desses anos que eu estou no grupo. Eu os agradeço, na pessoa da Dr. Cláudia Lima, pelo ótimo ambiente de trabalho e pela valiosa ajuda durante todo esse período. Em especial agradeço a minha querida Ilda, pela alegria contagiante, é impossível ficar triste ao seu lado! À Christina, minha querida tia Chris, pela convivência sempre tão prazerosa, pela disposição em nos ajudar e por toda a sua eficiência. Ao meu amigo Fernando pelo apoio e pelas longas conversas, sempre muito enriquecedoras. Aos queridos Adélia, Gabi e Daniel, companheiros de jornada, eu agradeço pelo prazer da convivência e pelos laços de amizade e confiança construídos no dia-a-dia. À querida Ana Cristina, meu braço direito (e esquerdo também) por toda a ajuda na parte experimental, por sua dedicação e eficiência!

Agradeço ao Curso de Pós-Graduação em Engenharia Metalúrgica e de Minas e às agências financiadoras: CNPq, INCT-Acqua, Fapemig e CAPES, pela oportunidade e

suporte durante todo este projeto. A toda equipe do Laboratório de Análises Químicas, em especial ao Dr. Júlio Silva e Drª Roberta Froes. Aos funcionários do Departamento de Engenharia Metalúrgica e de Materiais e do Curso de Pós-Graduação em Engenharia Metalúrgica e de Minas. Em especial, agradeço a Andréia do Laboratório de Difração de raios-X, Patrícia do Laboratório de Microscopia Eletrônica, e Maria Aparecida e Nelson do CPGEM por toda colaboração e convivência prazerosa.

Ao casal Airton e Mônica, os “culpados” por eu vir parar nesse grupo de pesquisa, agradeço a confiança, amizade e carinho que nos une desde os meus tempos de aluna do ensino técnico no Coltec.

À Professora Maria Sylvia, ou simplesmente Sica, pela disposição e entusiasmo em me ajudar, seja no laboratório de Raman, em sua sala, e até mesmo nas longas viagens ao LNLS. Ao Professor Igor F. Vasconcelos pela disposição em integrar esse projeto, saindo de Fortaleza exclusivamente para acompanhar meus experimentos no LNLS; e por todas as suas valiosas contribuições durante as análises por XAFS, tanto na aquisição dos dados como no tratamento dos mesmos. Ao Professor Hélio A. Duarte e ao Dr. Augusto Oliveira, pela colaboração no estudo do mecanismo de sorção de As(III) em gibbsita, uma parceria muito bem sucedida, mais uma vez, entre teoria e experimentos que tenho certeza ainda vai render muitos outros frutos. Ao Professor Jaime Mello e ao Dr. Juscimar Silva por gentilmente nos fornecerem as amostras de gibbsita sintética, viabilizando essa parte do projeto. To Professor James Kubicki at The Pennsylvania State University, for the receptiveness to me and to my project when I arrived there, and for all the valuable contributions during the theoretical modeling of As(III) immobilization on hematite.

To Professor Osseo-Asare, my co-advisor, for each wise advice, for all the support when I was at The Pennsylvania State University, for the example of professional, for trusting me, and mainly, for the privilege to call you my father and grandfather in my academic life.

Agradeço à minha orientadora, Professora Virginia Ciminelli, por todo o suporte, confiança e liberdade a mim concedidos. Pelo exemplo de profissional dedicada, exigente e, não por acaso, vitoriosa. Agradeço por me incentivar a buscar sempre o que há de melhor para complementar minha formação e por insistir para eu escrever sempre em inglês - você uma vez me disse que eu ainda a agradeceria por tal exigência e de fato aqui estou eu fazendo isso. Encerro, agradecendo pelo privilégio de fazer parte de um grupo de excelência em pesquisa, com o qual eu espero poder contribuir muito ainda.

SUMMARY

LIST OF FIGURES

LIST OF TABLES

LIST OF ACRONYMS

ab: acid-base sorption mechanism

AMD: Acid mine drainage

bb: bidentate-binuclear

bm: bidentate-mononuclear

DFT: Density functional theory

EXAFS: Extended X-ray absorption fine structure spectroscopy

IR: Infrared Spectroscopy

mb: monodentate-binuclear

MD: molecular dynamics

mm: monodentate-mononuclear

nd: non-dissociative sorption mechanism

PES: Potential energy surface

R = Interatomic distance

SCC-DFTB: Self-consistent charge corrected density-functional based tight-binding

XAFS: X-ray absorption fine structure spectroscopy

XANES: X-ray absorption near edge structure

RESUMO

Os mecanismos de imobilização de As(III) em gibbsita e hematita foram avaliados em função do pH e níveis de carregamento, respectivamente. Para o sistema As(III)-gibbsita, cálculos teóricos e EXAFS foram combinados para elucidar as estruturas dos complexos de As(III). Vários complexos de adsorção foram avaliados através do método "self-consistent charge corrected density-functional based tight-binding" (SCC-DFTB). O complexo bidentado-binuclear/acido-base (bb/ab) foi a geometria mais estável encontrada para a ligação do As(III) em gibbsita com As-O e As-Al distâncias de 1,75 e 3,24 Å respectivamente. Resultados de EXAFS confirmaram as estimativas do SCC-DFTB, mostrando 3 átomos de oxigênio na primeira camada a uma distância de 1,77 Å, e 2 de alumínio na segunda camada a uma distância de 3,21 Å, em todos os pH avaliados (5, 7 e 9). Em relação ao As(III) em hematita, o mecanismo foi elucidado combinando Raman, EXAFS e cálculos teóricos. Análises Raman foram realizadas primeiramente em amostras de hematita com diferentes níveis de carregamento de As(III) (variando de 0,005 mmol m^{-2} a 0,014 mmol m^{-2}) em pH 7,0. Cálculos teóricos foram realizados considerando diferentes possibilidades de ligação do As(III) em hematita, incluindo complexos monodentados e bidentados e a precipitação de claudetita, uma fase monoclínica de As_2O_3, na superfície do mineral. Esta última foi a configuração que melhor elucidou os resultados de Raman e, por isso, foi usada como modelo para ajustar os dados de EXAFS. Resultados de EXAFS demonstraram que As(III) pode formar um precipitado tipo claudetita na superfície da hematita com 3 átomos de oxigênio a uma distância de 1,74 Å, 2 átomos de arsênio a uma distância de 3,28 Å, e 2 átomos de ferro em uma distância de 3,54 Å. Nossos resultados mostraram que: (i) assim como o As(V), o As(III) preferencialmente se liga à gibbsita por meio de complexação tipo "inner-sphere", em pH de 5 a 9, suportando a hipótese de que a maior mobilidade do As(III) é relacionada ao caráter reversível da reação na superfície dos óxidos e não à fraqueza dessas interações. Com base nesta premissa, este trabalho também sugere um mecanismo de remobilização de As(III), quando a adsorção é o principal mecanismo de fixação, por meio da protonação do complexo bb/ab em meio ácido, liberando a molécula neutra H_3AsO_3; (ii) a viabilidade da precipitação de claudetita em hematita pode explicar os espectros Raman semelhantes do As(III) e As(V) em oxi-hidróxidos de Fe e mostra que as espécies de As(III) podem precipitar mesmo na presença de Fe(III) somente. Portanto, o presente trabalho melhora o entendimento das interações de As(III) com oxi-hidróxidos de alumínio e ferro. Finalmente, a partir de nossos resultados foi possível sugerir alternativas para controlar a mobilidade de As(III) em solos ricos em Al e Fe.

ABSTRACT

The mechanisms of aqueous As(III) species immobilization on gibbsite and hematite have been evaluated as a function of pH and coverage level, respectively. For the As(III)-gibbsite system, theoretical calculations and X-ray absorption fine structure spectroscopy (XAFS) were combined to elucidate the structure of arsenite surface complexes on the synthetic oxide. Several adsorption complexes have been evaluated using the self-consistent charge corrected density-functional based tight-binding (SCC-DFTB) method The bidentate-binuclear/acid-base complex (bb/ab) was found as the most stable geometry for As(III) bonding to gibbsite, showing As-O and As-Al distances of 1.75 and 3.24 Å, respectively. EXAFS results confirmed SCC-DFTB estimates with 3 oxygen atoms in the first shell, at a distance of 1.77 Å, and to 2 aluminum atoms in the second shell, at a distance of 3.21 Å, in a bidentate-binuclear configuration, at all pH evaluated (5.0, 7.0 and 9.0). Regarding the As(III) on hematite, the mechanism was elucidated by combining spectroscopic data (Raman and EXAFS) with theoretical calculations. Raman analyses were first carried out in samples of hematite with different As(III) coverage levels (varying from 0.0045 mmol m^{-2} to 0.014 mmol m^{-2}) at pH 7.0. Theoretical calculations were then performed considering different possibilities for As(III) linkage on hematite, including monodentate and bidentate sorption complexes and the precipitation of claudetite, a monoclinic As_2O_3 phase, on the mineral surface. This later was the configuration that best elucidated Raman results, and thus it was used as a model to fit the EXAFS data collected for As(III) immobilized on hematite at the same conditions used in Raman analyses. EXAFS results confirmed the calculations, demonstrating that As(III) may form a claudetite-like precipitated on the surface of hematite with 3 oxygen atoms at a distance of 1.74 Å, 2 arsenic atoms at a distance of 3.28 Å, and 2 iron atoms at a distance of 3.54 Å. Our results demonstrated that: (i) like As(V), As(III) species preferably link to gibbsite by means of inner-sphere complexation, in a pH range of 5-9, supporting the hypothesis that As(III) mobility is related to the reversible character of As(III) surface reactions rather than to the weakness of these interactions. Based on this premise, this work also suggested a mechanism for As(III) remobilization from oxides, when adsorption is the main mechanism of fixation, by means of protonation of the bb/ab adsorbed complex at acidic media, releasing the neutral H_3AsO_3 molecule; (ii) the feasibility of a claudetite-like precipitation on hematite could explain the similar Raman spectra for As(III) and As(V) species on iron oxy-hydroxides and show that As(III) species may precipitate in the presence of Fe(III) species only. Therefore, the present work improves the knowledge about the mode of As(III) interactions with aluminum and iron oxy-hydroxides. Finally, from our results it was possible to suggest alternatives to control As(III) mobility in Al and Fe-rich soils.

CHAPTER 1. INTRODUCTION

Arsenic is a toxic metalloid that occurs in several different minerals, usually in association with transition metals such as Au, Ag, and Cu. The greatest concentrations of As-bearing minerals occur in mineralized areas and among them, arsenopyrite (FeAsS) is the most abundant arsenic source (Mandal and Suzuki, 2002; Smedley and Kinniburgh, 2002). Regarding arsenic speciation in aqueous environments, it is mainly found in inorganic forms derived from arsenous acid (H_3AsO_3, $H_2AsO_3^-$, $HAsO_3^{2-}$ and AsO_3^{3-}) and arsenic acid (H_3AsO_4, $H_2AsO_4^-$, $HAsO_4^{2-}$ and AsO_4^{3-}). As is shown in Figure 1.1, under oxidizing conditions the predominant species is As(V), which is mainly present in the form of the oxyanions $H_2AsO_4^-$ and $HAsO_4^{2-}$. On the other hand, under slightly reducing conditions, As(III) is the thermodynamically stable species, present as neutral H_3AsO_3, in a wide pH range (pKa_1 H_3AsO_3 = 9.2). With respect to the organic arsenic species, the main forms are those derived from the dimethylarsinic acid, $DMA_{(III)}$ and $DMA_{(V)}$ ($(CH_3)_2AsOH$ and $(CH_3)_2OAsOH$, respectively) and from the monomethylarsonic acid, $MMA_{(III)}$ and $MMA_{(V)}$ ($CH_3AsO_2H_2$, and $CH_3AsO_3H_2$, respectively). These species are generally produced by biological activity and are rarely quantitatively important. However, the presence of these organic arsenic forms is becoming more significant in areas where waters are considerably impacted by industrial pollution.

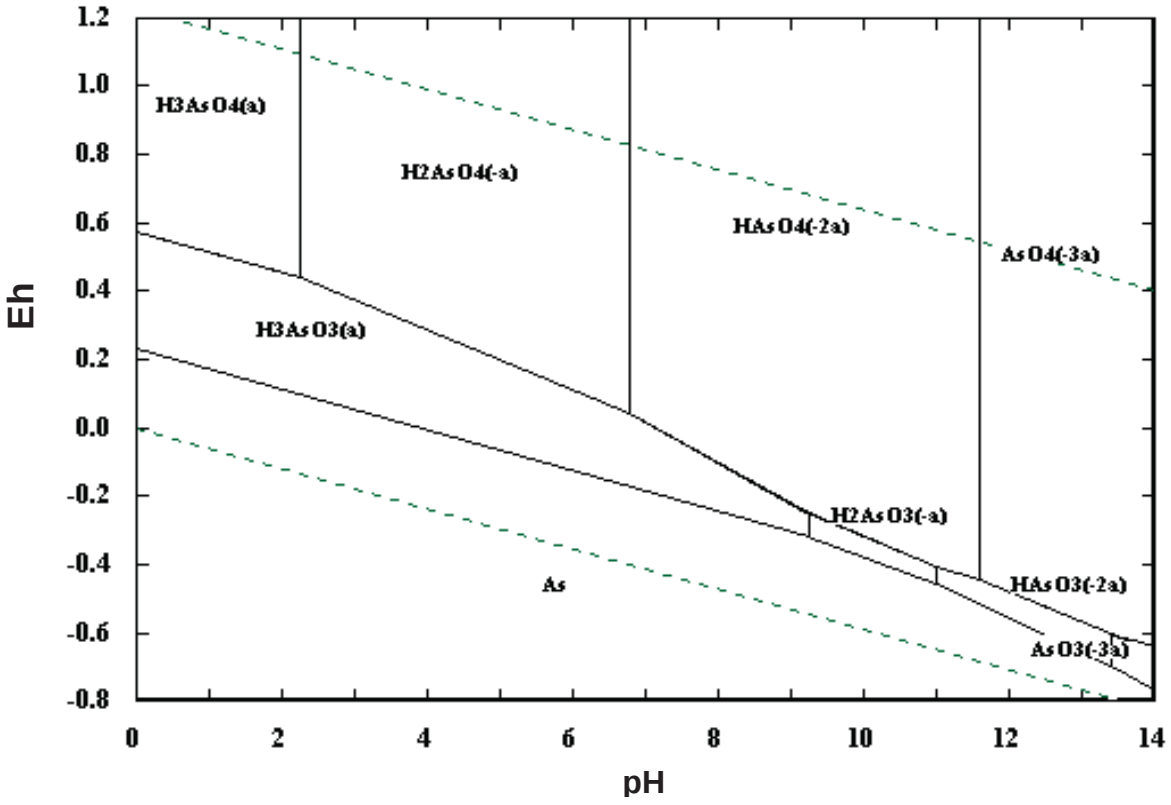

Figure 1.1: Eh-pH diagram for arsenic species in the As-H_2O system at 25ºC and $As_{molality}$= 0.1mol.kg^{-1} (obtained using the software HSC Chemistry 6.0).

Arsenic is a significant environmental contaminant worldwide, and its occurrence is mainly a result of natural processes, such as weathering reactions, biological activity and volcanic emissions. In terms of the population exposed, the arsenic incidence in groundwaters from Bangladesh, India, Taiwan, and China represent the most serious occurrences identified globally. In all these cases the groundwater used for human consumption showed a strong reducing condition, and the natural As(III) mobilization was pointed out as the main reason for the groundwater contamination (Smedley and Kinniburgh, 2002; Mandal and Suzuki, 2002).

Besides the natural occurrence, anthropogenic activities such as mining operation, pesticide manufacturing and application, petroleum refining, and burning of fossil fuels are potential sources for arsenic release to aqueous environments (Roussel *et al.,* 2000; Ning, 2002; Morín and Calas, 2006). Regarding the environmental contamination due to mining activities, arsenic can be released by the oxidation of sulfide minerals such as arsenopyrite (FeAsS) during the industrial roasting step or through acid mine drainage

(AMD), appearing as one of the main problems in mining areas (Williams, 2001; Ladeira and Ciminelli, 2004; Ritcey, 2005; Andrade *et al*., 2008). In Brazil, the main occurrence of arsenic is associated with gold mining, as in the region of the Iron Quadrangle and in the Paracatu district in Minas Gerais State, and in the metallurgy of copper concentrates (Matschullat *et al*., 2000; Borba *et al*., 2003; Deschamps *et al*., 2003; Mello *et al*., 2006; Andrade *et al*., 2008, Bundschuh *et al*., 2010).

Arsenic toxicity is strongly dependent on its oxidation state. The As(III) species are known to be 10 times more toxic than the As(V) species, and 70 times more toxic than the organic arsenic species (Kumaresan and Riyazunddin, 2001). Due to its high toxicity, environmental regulations are becoming increasingly more stringent with respect to the disposal of industrial arsenic-containing wastes. Therefore, arsenic removal from wastewater is often required before its disposal. The development of technologies for arsenic removal from industrial wastewater and contaminated drinking water has been the subject of several studies in the last decades. The main efforts have been directed at reaching an efficient immobilization of the arsenic, which means to generate chemically stable arsenic products to be safely disposed of in adequately prepared landfills or tailings dams. As a consequence, due to As(III) higher mobility compared to As(V) species, when it is present in the media, an oxidation step is often demanded before the wastewater treatment to guarantee the As(V) as the predominant arsenic species in the system. Thus, the consolidated methodologies available currently are based on the processes of As(V) precipitation with iron, and arsenic sorption on iron, manganese and aluminum oxy-hydroxides (Harris, 2003; Bundschuh *et al*., 2010).

1.1 Arsenic sorption on iron and aluminum oxy-hydroxides

The oxy-hydroxides of iron and aluminum are particularly significant minerals related to arsenic immobilization in aqueous environment. The strong affinity of arsenic for these minerals, i.e., the ability of Fe and Al oxy-hydroxides to immobilize arsenic species, is invoked as an important mechanism of its natural attenuation in soils, groundwater and sediments (Smedley and Kinniburgh, 2002; Vasconcelos *et al.,* 2004; Silva *et al.,* 2007). As a consequence, the performance of iron and aluminum oxy-hydroxides, such as goethite (α-FeO-OH), lepidocrocite (γ-FeO-OH), ferrihydrite (FeO-OH), hematite (α-Fe_2O_3), amorphous Al hydroxide ($Al(OH)_3$), and gibbsite (crystalline $Al(OH)_3$), has been extensively evaluated in the past few decades for arsenic removal from aqueous

environments (Manning and Goldberg, 1997; Raven *et al.*, 1998; Jain *et al.*, 1999; Goldberg and Johnston, 2001; Goldberg, 2002; Dixit and Hering, 2003; Ladeira and Ciminelli, 2004; Silva *et al.,* 2007; Al-Abed *et al*., 2007; Mohan and Pittman, 2007). It has been found in these afore mentioned works that both As(V) and As(III) species can be retained by these minerals. However, these two arsenic species present very different sorption behaviors. Usually, the As(V) species presents a higher sorption affinity at acid environment (pH around 4). The opposite happens with the As(III), which is more efficiently sorbed at higher pH values (between 7 and 9).

Regarding the molecular mechanisms of arsenic immobilization, the structures of the complexes formed during arsenic sorption on the surfaces of iron and aluminum oxy-hydroxides have been extensively studied using X-ray absorption spectroscopy (XAS). Waychunas *et al.* (1996) and Fendorf *et al*. (1997) have found that the major mechanism for As(V) adsorption on goethite and ferrihydrite is through the formation of a bidentate binuclear complex, though some monodentate complexes were also observed. According to Fendorf *et al.* (1997), different surface coverage levels may cause the formation of different complexes. Farquhar *et al.* (2002) investigated the mechanisms whereby As(V) and As(III) in aqueous solution (pH 5.5-6.5) interact with the surfaces of goethite (α-FeO-OH) and lepidocrocite (γ-FeO-OH) using EXAFS and XANES analyses. The arsenic species was shown to remain in the original oxidation state with the first shell coordinated to four oxygens at 1.78 Å for As(III) and 1.69 Å for As(V). These authors also found that inner sphere bidentate complexes are formed for both arsenate, As(V), and arsenite, As(III) species. Sherman and Randall (2003) studied the mechanism of As(V) adsorption on various ferric oxyhydroxides, demonstrating that the adsorption of arsenate $H_nAsO_4^{3-n}$ onto goethite, lepidocrocite, hematite and ferrihydrite occurs by the formation of inner-sphere surface complexes resulting from bidentate corner-sharing between AsO_4 and FeO_6 polyhedra.

Regarding the aluminum oxy-hydroxides, Ladeira *et al.* (2001), through XAS analyses and DFT calculations, showed that As(V) forms preferably an inner sphere bidentate binuclear complex on the gibbsite surface. During these calculations, three other different sorption sites in which arsenate can interact with gibbsite were also considered (bidentate mononuclear, monodentate mononuclear, and monodentate binuclear complexes), however their formation was shown to be less favorable. Kubicki (2005) has performed theoretical calculations for the As(III) and As(V) bonding on Al and Fe hydroxides surfaces. The author has considered both monodentate and bidentate complex

configurations, and the obtained results were then compared to the interatomic distances derived from EXAFS and the vibrational frequencies from IR and Raman analyses. The calculated results indicated that the bidentate complex configuration is most consistent with spectroscopic data found in the literature (Tossell, 1997; Ladeira *et al.*, 2001; Sherman and Randal, 2003). However, based on the model Gibbs free energies of adsorption, the monodentate configuration is suggested as the most stable configuration.

As can be seen from the above, most of these studies have focused on As(V) immobilization, allowing a conclusive understanding about the interactions of the pentavalent arsenic with the surface of many oxide minerals. Regarding As(III) immobilization mechanisms, Manning *et al*. (1998) evaluated the sorption of As(III) on goethite and suggested that As(III) formed bidentate, binuclear surface complexes on iron oxy-hydroxides. Ona-Nguema *et al*. (2005) have investigated the As(III) sorption onto two-line ferrihydrite, hematite, goethite, and lepidocrocite under anoxic condition. The obtained results presented some discrepancies concerning goethite and lepidocrocite experiments with regard to the nature of the secondary complex that contributes to As(III) sorption, when compared to previous works. While Manning *et al*. (1998) and Farquhar *et al*. (2002) have observed only bidentate-binuclear (bb) complexes for As(III) sorbed on goethite at very low surface coverage, Ona-Nguema *et al*. (2005) found that, although “bb” complexes predominate, a minor monodentate mononuclear (mm) surface complex is also present. Regarding the As(III) on lepidocrocite, both Manning *et al*. (1998) and Farquhar *et al*. (2002) found a contribution of the bidentate-binuclear and bidentate-mononuclear (bm) complexes. The Ona-Nguema *et al*. (2005) results disagree with importance of the “bm” complexes, showing a major contribution of the “bb” and “mm” surface complexes for the As(III)-sorbed lepidocrocite sample. Concerning ferrihydrite and hematite experiments, the work by Ona-Nguema *et al*. (2005) was the first one that assessed the As(III) immobilization mechanisms onto these minerals. The authors have found that “bb” and “bm” complexes are important for As(III) immobilization on both hematite and ferrihydrite surfaces, and they suggested the use of DFT calculations in order to confirm among these complexes which would be the most stable one. However, their experiments were carried out at anoxic condition, while in the present work the experiments were carried out in the presence of oxygen.

More recent investigations of arsenic-iron systems under anoxic conditions have indicated that As(III) tends to form polymeric complexes and precipitates on the surface of Fe(II,III) oxy-hydroxides. Wang *et al*. (2008) suggested by means of EXAFS analyses that As(III)

forms surface precipitates at high surface coverage on magnetite nano-particles, while monomeric surface complexes with tridentate geometry would be formed at low surface coverage. The formation of As(III) oligomeric species at the surface of $Fe(OH)_2$ and green-rusts was also proposed by Ona-Nguema *et al*. (2009) and Wang *et al*. (2010).

Additionally, some studies on As(III) immobilization onto different aluminum mineral phases have shown conflicting results. Goldberg and Johnston (2001) have found that As(III) exhibits only a weak affinity for amorphous Al_2O_3, resulting in the formation of an outer-sphere complex. In opposition, Arai *et al*. (2001) determined that As(III) forms predominantly an inner-sphere bidentate binuclear complex on γ-Al_2O3, at pH 5.5. Weerasooriya *et al*. (2003) proposed that As(III) forms outer-sphere surface complex with gibbsite surface, based on the sorption ionic strength and pH dependences. Oliveira *et al*. (2006) used density functional methods and cluster models to study two different mechanisms for the H_3AsO_3 immobilization on gibbsite (γ-$Al(OH)_3$. The results showed that, differently from the As(V) case, As(III) is not retained through an acid/base, but by a non-dissociative mechanism in which O-H bonds are not being broken and act as a link to the two metal centers. According to the authors, this non-dissociative mechanism can reconcile the high remobilization of As(III) with the apparently inconsistent formation of inner-sphere adsorption complexes. However, we are not aware of experimental data supporting this proposed mechanism.

Our research group has been extensively studying the mechanisms of arsenic immobilization onto iron and aluminum compounds. Regarding As(V), it was well established the mechanisms of its sorption onto gibbsite using EXAFS analyses and DFT calculations (Ladeira *et al*., 2001), and onto a Mn-Fe mineral-containing soil using XANES analyses (Deschamps *et al.,* 2003). On the other hand, concerning As(III) sorption, the obtained results did not allow to reach a conclusive explanation about the structure of the formed complexes. Ladeira *et al.* (2004), have suggested that both outer and inner-sphere complexes can be formed during the As(III) sorption onto a natural gibbsite. The outer-sphere complex formation was correlated with the elevated concentrations of soluble As(III) obtained by leaching with different aqueous solutions, and the relatively higher mobility of As(III) in natural systems. However, preliminary spectroscopy data obtained by these authors for As(III) loaded onto natural gibbsite pointed to the existence of inner-sphere neutral complexes at pH 5.5. In another work, Müller (2006) and Müller *et al.* (2010) investigated the surface complexes of As(III) and As(V) on ferrihydrite, feroxyhyte, goethite and hematite with Raman and Infrared spectroscopy. Raman data of As(III)

adsorption onto the studied iron oxides provided very similar features to those of As(V) adsorption, a band centered near to 860cm^{-1}. In order to verify the As(III) oxidation hypothesis, IR spectroscopy and XANES analyses were carried out. IR results showed different As(III) and As(V) iron oxides spectra. If the hypothesis of oxidation were true, these spectra should be similar. Furthermore, XANES measurements confirmed that As(III) was not oxidized to As(V) during the immobilization. Therefore, it was not possible to fully elucidate the structure of the As(III) complexes formed on the surface of the iron oxides as indicated by Müller *et al.* (2010).

As shown above, important uncertainties still remain with regard to the structure of the trivalent arsenic complexes on the mineral surfaces in aqueous environments. Therefore, considering the aforementioned context, the present work is aimed at studying the mechanisms of trivalent arsenic fixation on iron and aluminum oxy-hydroxides surfaces. The investigation is aimed to advance the understanding of As(III) interactions with these common substrates found in natural systems as well as their implications on arsenic mobility in the environment. For these purposes, the molecular mechanisms whereby As(III) immobilization on gibbsite and hematite take place were evaluated. The structures of the complexes formed on these mineral surfaces were determined by combining XAFS, Raman spectroscopy and theoretical calculations. As important outcomes of this work we can highlight the determination of the structural environment of As(III) on gibbsite and hematite, which improves the knowledge about the mode of As(III) interactions with aluminum and iron oxy-hydroxides. Consequently, our results provide helpful information to predict and control arsenic mobility in environments where Fe and Al oxy-hydroxides are often found.

1.2 Relevance and Objectives

It is well known that the natural attenuation of the arsenic species is closely related to their interactions with the iron and aluminum oxy-hydroxides present in soils, either by adsorption or precipitation on these mineral surfaces. A practical evidence of the contribution of both sorption and precipitation processes during arsenic immobilization on soils has been observed at Kinross gold company, where soil liners containing iron and aluminum oxy-hydroxides are applied as natural barriers in tailings dam used for disposal of sulfide concentrates. According to the company's monitoring report, the enriched-iron and aluminum clay materials have acted as an efficient natural barrier for tailings seepage of solutions containing relatively high concentrations of arsenic, sulfates, cyanide and trace metals during almost 2 decades. This long-term arsenic removal from the wastewater as well as macroscopic evidences obtained from the observation of secondary phases formed on the most external layers suggest that adsorption is not the only process involved in As immobilization.

The majority of the studies that have been carried out regarding the arsenic immobilization mechanisms have focused on the As(V) species, allowing a conclusive understanding about the interactions of the pentavalent arsenic with the surface of many oxide minerals. On the other hand, as previously shown in the Introduction section, the mechanism of As(III) immobilization have lately been the focus of some significant investigations, however it is still controversial. Since the As(III) is the most common arsenic species at reducing environments, which is the usual condition in groundwaters and also in the deeper regions of tailings dams, a conclusive understanding about its behavior must be reached in order to be able to control arsenic immobilization processes in a long term basis.

In this context, the present work is aimed at evaluating the As(III) interactions with iron and aluminum oxy-hydroxides in order to elucidate its mechanisms of immobilization. The understanding of As(III) interactions with iron and aluminum oxy-hydroxides requires the knowledge of the immobilization mechanisms at a molecular level, since the structural environment of arsenic at the mineral surface may determine its fixation and, consequently, the potential for remobilization. Therefore, the combination of X-ray Absorption Spectroscopy (XAS), vibrational techniques (Raman spectroscopy), and

theoretical modeling must be considered as a powerful approach to achieve the goals of the present work. The following specific objectives were pursued in this work:

(i) to characterize the sorption complexes formed during As(III) immobilization on gibbsite by means of theoretical calculations and XAFS analyses;

(ii) to characterize the sorption complexes formed during As(III) immobilization on hematite by combining Raman spectroscopy, theoretical modeling and XAFS analyses;

(iii) to infer about the implications of the structures of the complexes formed during As(III) immobilization on gibbsite and hematite on the arsenic mobility in the environment.

1.3 Thesis structure and organization

The present Thesis was organized in 5 chapters. In the Chapter 1 the work was contextualized by means of a critical review of the main, few works found in the literature, where is highlighted the major lacks regarding the study of the mechanisms for As(III) sorption on iron and aluminum oxy-hydroxides. The relevance and objectives, as well as the main contributions of the project were also presented in Chapter 1. In Chapter 2 and Chapter 3, the main results achieved during this Thesis work are presented and discussed.

Chapter 2 evaluated the mechanism of As(III) sorption on gibbsite by combining XAS analyses and DFT calculations. This chapter originated the paper "As(III) immobilization on gibbsite: investigation of the complexation mechanism by combining EXAFS analyses and DFT calculations", *Geochimica and Cosmochimica Acta* (2012), vol. 83 205–216. Theoretical calculations were done in collaboration with Dr. Helio Anderson Andrade and Dr. Augusto Faria Oliveira, from Universidade Federal de Minas Gerais (UFMG) and Technische Universität Dresden - Germany, respectively. XAFS measurements and data analyses were performed in collaboration with Dr. Igor Frota Vasconcelos from Universidade Federal do Ceará.

Chapter 3 presents the evaluation of the mechanisms for As(III) sorption on hematite by combining X-ray Absorption Spectroscopy, Raman Spectroscopy, and theoretical modeling. This chapter originated the paper "Evidences of a new surface oligomer for As(III) complexation on hematite from Raman spectroscopy, DFT calculations, and EXAFS", submitted to the Journal *Environmental Science and Technology*. Raman analyses were carried out at the Department of Metallurgical and Materials Engineering-UFMG, orientated by Drª Maria Sylvia Dantas. Theoretical modeling was performed in collaboration with Dr. James D. Kubicki and Dr. Heath D. Watts from The Pennsylvania State University - USA. XAFS measurements and data analyses were performed in collaboration with Dr. Igor Frota Vasconcelos from Universidade Federal do Ceará.

Chapter 4 highlights the implications from the results reported in Chapters 2 and 3 for As mobility. Finally, Chapter 5 brings the final considerations of the project, including the main conclusions, the original contributions from the Thesis, and the suggestions to future works.

1.4 References

AL-ABED, S. R.; JEGADEESAN, G.; PURANDARE, J. and ALLEN, D. (2007). Arsenic release from iron rich mineral processing waste: Influence of pH and redox potential. *Chemosphere*, vol. 66, p. 775 - 782.

ANDRADE, R. P.; FIGUEIREDO, B. R.; MELLO, J. W. V.; SANTOS, J. C. Z., and ZANDONADI L. U. (2008). Control of Geochemical Mobility of Arsenic by Liming in Materials Subjected to Acid Mine Drainage. *Journal of Soils and Sediments*, vol. 8 (2), p. 123-129.

ANDRADE, R. P.; FILHO, S. S., MELLO, J. W. V; FIGUEIREDO, B. R., and DUSSIN, T. M. (2008). Arsenic mobilization from sulfidic materials from gold mines in Minas Gerais state. *Química Nova*, vol. 31 (5), p. 1127-1130.

ARAI, Y., ELZINGA, E. and SPARKS, D.L., (2001). X-ray absorption spectroscopic investigation of arsenite and arsenate adsorption at the aluminum oxide–water interface. *Journal of Colloid Interface Science*. vol. 235, p. 80 - 88.

BORBA, R. P.; FIGUEIREDO, B.R.; RAWLINS, B., and MATSCHULLAT, J. (2003). Geochemical distribution of arsenic in waters, sediments and weathered gold mineralized rocks from Iron Quadrangle, Brazil. *Environmental Geology, 44, (1),39-52.*

BUNDSCHUH, J.; LITTER, M.; CIMINELLI, V. S. T.; MORGADA, M. E.; CORNEJO, L.; HOYOS, S G.; HOINKIS, J.;. ALARCON-HERRERA, M. T.; ARMIENTA, M. A., and BHATTACHARYA, P. (2010). Emerging mitigation needs and sustainable options for solving the arsenic problems of rural and isolated urban areas in Latin America - A critical analysis. *Water Research, In press.*

DESCHAMPS, E.; CIMINELLI, V. S. T.; WEIDLER, P. G. and RAMOS, A Y. (2003). Arsenic sorption onto soils enriched in Mn and Fe minerals. *Clays and Clay Minerals*, vol. 51, p. 197-204.

DIXIT, S. and HERING, J. G. (2003). Comparison of Arsenic(V) and Arsenic(III) Sorption onto Iron Oxide Minerals: Implications for Arsenic Mobility. *Environmental Science and Technology,* vol. 37, p. 4182-4189.

FARQUHAR, M.L.; CHARNOCK, J.M.; LIVENS, F.R. and VAUGHAN, D.J. (2002). Mechanisms of arsenic uptake fom aqueous solution by interaction with goethite, lepidocrocite, mackinawite, and pyrite: an X-ray absorption spectroscopy study. *Environmental Science and Technology*, vol. 36, p. 1757–1762.

FENDORF, S.; EICK, M.J.; GROSSL, P. and SPARKS, D.L. (1997). Arsenate and chromate retention mechanisms on gothite. 1. surface structure. *Environmental Science and Technology,* vol. 31, (2), p. 320.

GOLDBERG, S., (2002). Competitive adsorption of arsenate and arsenite on oxides and clay minerals. *Soil Sci. Am. J.* vol. 66, p. 413–421.

GOLDBERG, S. and JOHNSTON, C.T. (2001). Mechanisms of arsenic adsorption on amorphous oxides evaluated using macroscopic measurements, vibrational spectroscopy, and surface complexation modeling. *Journal of Colloid Interface Science*, vol. 234, p. 204–216.

HARRIS, G.B. (2003). The removal of arsenic from process solutions: theory and industrial practice. *In: Hydrometallurgy 2003 – In: Hydrometallurgy 2003 – International Conference in Honor of Prof. Ian Ritchie; TMS,* Warrendale, PA - USA; vol. 2.

HSC Chemistry, (2007) Chemical Reaction and Equilibrium Software with Extensive Thermochemical Database. Version 6.12, Outokumpu Research Oy, Piori, Finland.

JAIN, A., RAVEN, K.P. and LOEPPERT, R.H. (1999). Arsenite and arsenate adsorption on ferrihydrite: surface charge reduction and OH- release stoichiometry. *Environmental Science and Technology,* vol. 33, p. 1179–1184.

KUBICKI, J.D. (2005). Comparison of As (III) and As (V) complexation onto Al and Fe-hydroxides. *In: Advances in Arsenic Research: Integration of Experimental and Observational Studies and Implications for Mitigation* .Eds P. O'Day, D. Vlassopoulos and L. Benning, ACS Symposium Series, 915, p. 104-117, Washington DC.

KUMARESAN, M. and RIYAZUNDDIN, P. (2001). Overview of speciation chemistry of arsenic. *Current Science*, vol. 80, p. 837-846.

LADEIRA, A. C. Q.; CIMINELLI, V. S. T.; DUARTE, H. A.; ALVES, M. C. M. and RAMOS, A. Y. (2001). Mechanism of anion retention from EXAFS and density functional calculations: Arsenic (V) adsorbed on gibbsite. *Geochimica et Cosmochimica Acta,* vol. 65, p. 1211–1217.

LADEIRA, A. C. Q. and CIMINELLI, V. S. T. (2004). Adsorption and desorption of arsenic on an oxisol and its constituents. *Water Research*, vol. 38, p. 2087 – 2094.

MANDAL, B. K. and SUZUKI, K. T. (2002). Arsenic round the world: a review. *Talanta,* vol. 58, p. 201-235.

MANNING, B.A.; FENDORF, M. and GOLDBERG, S., (1998). Surface structures and stability of arsenic(III) on goethite: spectroscopic evidence for innersphere complexes. *Environmental Science and Technology,* vol. 32, p. 2383–2388.

MANNING, B.A. and GOLDBERG, S. (1997). Adsorption and stability of arsenic (III) at the clay mineral–water interface. *Environmental Science and Technology,* vol. 31, p. 2005-2011.

MATSCHULLAT, J.; Borba, R.P.; Deschamps, E.; Figueiredo, B.F.; Gabrio, T.; Scwenk, M. (2000). Human and environmental contamination in the Iron Quadrangle, Brazil. *Applied Geochemistry, 15, 181-190*.

MELLO, J.W.V.; Roy, W.R.; Talbott, J.L.; Stucki, J.W. (2006). Mineralogy and Arsenic Mobility in Arsenic-rich Brazilian Soil and Sediments. *J. Soils & Sediments*., vol. 6 (1), p. 9-19.

MOHAN, D. and PITTMAN, C. U. (2007). Arsenic removal from water/wastewater using Adsorbents - a critical review. *Journal of Hazardous Materials,* vol.142, p. 1-53.

MORÍN, E. G. and CALAS, G. (2006). Arsenic in soils, mine tailings, and former industrial sites. *Elements - Mineralogical Society of America*, vol. 2, p. 97-101.

MÜLLER, K. (2006). Investigation of the sorption of dissolved As compounds with spectroscopic methods. TU Dresden, Faculty of Forestry, Geosciences and Hydrosciences, Institute for Waste Management and Contaminated Site Treatment; Diploma thesis.

MÜLLER, K.; WILLSCHERA, S.; DANTAS, M. S. S., CIMINELLI, V. S. T. (2010). A comparative study of As(III) and As(V) in aqueous solutions and adsorbed on iron oxy-hydroxides by Raman Spectroscopy, *Water Research,* vol. 44, 5660 - 5672.

NING, R. Y. (2002). Arsenic removal by reverse osmosis. *Desalination,* vol. 143, p.237-241.

OLIVEIRA, A. F.; LADEIRA, A. C. Q.; CIMINELLI, V. S. T.; HEINE, T. and DUARTE, H. A. (2006). Structural model of arsenic(III) adsorbed on gibbsite based on DFT calculations. *Journal of Molecular Structure: THEOCHEM*, vol.762, p. 17 - 23.

ONA–NGUEMA, G.; MORIN, G.; JUILLOT, F.; CALAS, G. and BROWN Jr., G. E. (2005). EXAFS Analysis of Arsenite Adsorption onto Two-Line Ferrihydrite, Hematite, Goethite, and Lepidocrocite. *Environmental Science and Technology,* vol. 39, p. 9147 - 9155.

ONA–NGUEMA, G.; MORIN, G.; WANG, Y.; MENGUY, N.; JUILLOT, F.; OLIVI, L.; AQUILANTI, G.; ABDELMOULA, M.; RUBY, C.; BARGAR, J.R.; GUYOT, F.; CALAS, G. and BROWN Jr, G. E (2009). Arsenite sequestration at the surface of nano-$Fe(OH)_2$, ferrous-carbonate hydroxide, and green-rust after bioreduction of arsenic-sorbed lepidocrocite by *Shewanella putrefacien*. *Geochimica et Cosmochimica Acta*, vol. 73, p. 1359 - 1381.

RAVEN, K. P.; JAIN, A. and LOEPPERT, R. H. (1998). Arsenite and Arsenate Adsorption on Ferrihydrite: Kinetics, Equilibrium, and Adsorption Envelopes. *Environmental Science and Technology,* vol. 32, p. 344-349.

RITCEY, G. M. (2005). Tailings management in gold plants. *Hydrometalurgy,* vol. 78, p. 3-20.

ROUSSEL, C.; NÉEL, C. and BRILL, H. (2000). Minerals controlling arsenic and lead solubility in an abandoned gold mine tailings. The Science of the Total Environment, vol. 263, p. 209-219.

SHERMAN, D. and RANDALL, S. R. (2003). Surface complexation of arsenic(V) to iron(III) (hydr)oxides: Structural mechanism from ab initio molecular geometries and EXAFS spectroscopy. *Geochimica et Cosmochimica Acta*, vol. 67, nº. 22, p. 4223 - 4230.

SILVA, J;. MELLO, J. W.V; GASPARON, M., ABRAHÃO, W. A.P. and JONG, T. *(*2007). Arsenate adsorption onto aluminium and iron (hydr)oxides as an alternative for water treatment In: IMWA Symposium 2007: Water in Mining Environments, Eds: R. Cidu and F. Frau, Cagliari, Italy

SMEDLEY, P. L. and KINNIBURGH, D. G. (2002). A review of the source, behavior and distribution of arsenic in natural waters. *Applied Geochemistry,* vol. 17, p. 517 - 568.

TOSSELL, J.A. (1997). Theoretical studies on arsenic oxide and hydroxide species in minerals and in aqueous solution. *Geochimica Cosmochimica Acta*, vol. 61, p.1613-1623.

VASCONCELOS, F. M.; CIMINELLI, V. S. T.; OLIVEIRA, R. P., and SILVA, R. J. (2004). Determinação da especiação química e potencial de mobilidade do arsênio em sítios de mineração. *Geochimica. Brasiliensis,* vol. 18 , p. 115-120.

WANG, Y.; MORIN, G.; ONA–NGUEMA, G.; MENGUY, N.; JUILLOT, F.; AUBRY, E.; GUYOT, F.; CALAS, G., and BROWN Jr, G. E (2008) Arsenite sorption at the magnetite-water interface during aqueous precipitation of magnetite: EXAFS evidence for a new arsenite surface complex. *Geochimica et Cosmochimica Acta*, vol. 72, p. 2573 - 2586.

WANG, Y.; MORIN, G.; ONA–NGUEMA, G.; JUILLOT, F.; GUYOT, F.; CALAS, G., and BROWN Jr, G. E (2010). Evidence for different surface speciation of arsenite and arsenate on green rust: an EXAFS and XANES study. *Environmental Science and Technology*, vol. 44, p. 109 - 115.

WAYCHUNAS, G. A.; DAVIS, J. A. and FULLER C. C. (1996). Geometry of sorbed arsenate on ferrihydrite and crystalline FeOOH: Re-evaluation of EXAFS results and topological factors in predicting sorbate geometry, and evidence for monodentate complexes. *Geochimica et Cosmochimica Acta*, vol. 59, nº 17, p. 3655-3661.

WEERASOORIYA, R., TOBSCHALL, H. J., WIJESEKARA, H. K. D. K., ARACHCHIGE, E. K. I. A. K. U. K. and PATHIRATHNE, K. A. S. (2003). On the mechanistic modeling of As(III) adsorption on gibbsite. *Chemosphere*, vol. 51, p. 1001–1013.

WILLIAMS, M. (2001). Arsenic in mine waters: an international study. *Environmental Geology*, *40, (3), 267-278.*

CHAPTER 2. As(III) immobilization on gibbsite: investigation of the complexation mechanism by combining EXAFS analyses and DFT calculations

ABSTRACT

The complexation of aqueous As(III) species on gibbsite was investigated as a function of pH. Theoretical calculations and X-ray absorption fine structure spectroscopy (XAFS) were combined to elucidate the structure of arsenite surface complexes on synthetic gibbsite. Several adsorption sites were evaluated using the self-consistent charge corrected density-functional based tight-binding (SCC-DFTB) method. The formation of bidentate-binuclear, bidentate-mononuclear, monodentate-mononuclear, and monodentate-binuclear complexes by means of both acid-base and non-dissociative mechanisms was studied in detail. The SCC-DFTB calculations showed the bidentate-binuclear/acid-base complex as the most thermodynamically stable geometry for As(III) bonding to gibbsite surface, estimating As-O and As-Al distances of 1.75 and 3.24 Å, respectively. EXAFS results also demonstrated As(III) complexation to three oxygen atoms in the first shell, at a distance of 1.77 Å, and to aluminum in the second shell at a distance of 3.21 Å, characteristic of bidentate-binuclear configuration, at pH 5.0, 7.0 and 9.0. Another As-Al interaction, attributed to the monodentate-binuclear complex due to its distance of 3.49 Å, was shown from EXAFS results to provide a minor contribution to As(III) sorption on gibbsite. Therefore, results from theoretical calculations and experimental measurements confirmed the occurrence of inner-sphere complexation during the As(III) adsorption on gibbsite, in a pH range of 5-9. Hence, the higher As(III) mobility in the environment, when compared to As(V), was suggested to be related to the feasibility of protonation of the As(III) adsorbed complexes. This protonation would restore the neutral H_3AsO_3 molecule, which could be then released from the mineral surface. These results might be useful to predict and control arsenic mobility in aqueous environments, particularly where Al oxy-hydroxides are often found.

Key-words: Arsenite sorption, gibbsite, mechanism, EXAFS, DFT calculations

2.1 Introduction

Arsenic immobilization on iron and aluminum oxy-hydroxides has been the subject of much investigation in the past few decades (Hering *et al.,* 1997; Fendorf *et al.,* 1997; Manning *et al*., 1998; Goldberg and Johnston, 2001; Dixit and Hering, 2003; Ladeira and Ciminelli, 2004; Kubicki, 2005). Some of these studies have reported that iron oxy-hydroxides are more efficient for arsenic removal from aqueous solutions than the analogous aluminum phases. However, the higher arsenic uptake by Fe oxy-hydroxides may be a consequence of their usually higher specific surface area and not due to a significant difference in the capacity of iron and aluminum compounds to adsorb arsenic. When the solid's specific surface area is also considered, the differences in the arsenic uptake amongst the various iron oxide and oxy-hydroxides and aluminum hydroxide are not so evident. Corroborating with this observation, Silva et al. (2010) found that, on a weight basis, the maximum As(V) uptake by various minerals followed the sequence: Ferrihydrite (1.258 ± 0.034 mmol g^{-1}) > Gibbsite (0.228 ± 0.006 mmol g^{-1}) > Hematite (0.193 ± 0.006 mmol g^{-1}) > Goethite (0.101 ± 0.002 mmol g^{-1}). On the other hand, when the specific surface area of the solids was also taken into account, all the Fe and Al oxy-hydroxides tested reached a maximum adsorption capacity of approximately 0.005 mmol m^{-2}. An additional contribution of aluminum oxy-hydroxides to arsenic fixation comes from the fact that arsenic may be released eventually to the environment due to reductive dissolution of the Fe(III) oxy-hydroxides, while the solubility of Al(III) oxy-hydroxides is not as strongly affected by redox processes (Meng *et al*., 2001; Masue *et al*., 2007; Silva *et al.*, 2010).

Gibbsite, α-$Al(OH)_3$ (Saafeld and Wedde, 1974), is a particularly important aluminum oxy-hydroxide commonly found in abundance in tropical soils (Schaefer *et al.*, 2008; Macedo and Bryant, 1987), and it is known to play a significant role during arsenic natural attenuation in the environment (Ladeira and Ciminelli, 2004; Mello *et al.*, 2006). An important example is the work done by Mello *et al.* (2006), in which As-enriched soils and sediments from different mining regions of Brazil were investigated. The work shows that the low values of soluble As from the evaluated samples is related to the presence of gibbsite, a large amount of iron oxides, and a lack of organic matter in the solid phase. The environmental implications of the presence of gibbsite were also highlighted, since it is thermodynamically more stable than iron oxides under anaerobic conditions, such as those found in waterlogged soils and lake sediments. In another work, Pantuzzo and Ciminelli (2010) investigated arsenic association and the long-term stability of disposed

arsenic residues. The authors have found indications that, in addition to iron and calcium, arsenic was also associated to Al in the form of Al-arsenate co-precipitates in the residues aged for around 20 years. These findings corroborate our group's initial results on the main oxisol features responsible for As fixation in mining areas, which showed a good correlation between arsenic uptake and aluminum oxides content in the soil samples (Ladeira and Ciminelli, 2004). Hence, a better understanding about how arsenic species interact with aluminum hydroxides, especially gibbsite, is expected to advance the prediction and control of As distribution in aqueous environments (Ladeira *et al*, 2001; Arai *et al*., 2001; Weerasooriya *et al*., 2004).

Most of the previous work has focused on the As(V) species. In a convincing study, Ladeira *et al*. (2001) have elucidated the mechanism of As(V) immobilization on gibbsite. Results from Extended X-ray Absorption Fine Structure (EXAFS) analysis and Density Functional Theory (DFT) demonstrated that As(V) formed preferably an inner sphere bidentate-binuclear complex on the surface of Al oxy-hydroxyl octahedra at pH around 5. Regarding the trivalent arsenic species, there have been few studies focused on its immobilization on gibbsite. Weerasooriya *et al*. (2003) proposed that As(III) forms outer-sphere surface complexes on gibbsite surface, based on the ionic strength and pH dependences of the sorption. Ladeira and Ciminelli (2004) evaluated arsenic sorption/desorption behavior on an oxisol and its main constituents and they demonstrated a significant uptake of both As(V) and As(III) by gibbsite, respectively 4.6 mg g^{-1} and 3.3 mg g^{-1}. However, while only a maximum of 2% of the sorbed As(V) was leached from the selected samples, As(III) leaching reached up to 32% in the presence of sulfate ions. According to the authors, the formation of outer-sphere complexes would explain the relatively higher remobilization observed for As(III), compared to As(V) species. However, the authors affirmed that their preliminary spectroscopic data obtained for As(III) loaded onto natural gibbsite pointed to the existence of inner-sphere neutral complexes at pH 5.5. Some studies on As(III) immobilization onto different aluminum mineral phases have also shown divergent results. Goldberg and Johnston (2001) reported that As(III) exhibits only a weak affinity for amorphous Al_2O_3, resulting in the formation of an outer-sphere complex. In contrast, Arai *et al*. (2001) concluded that As(III) forms predominantly an inner-sphere bidentate binuclear complex on γ-Al_2O_3, at pH 5.5.

As can be seen from the above, there is no consensus about the mechanism of the As(III) immobilization on aluminum oxy-hydroxides. Furthermore, Ladeira and Ciminelli (2004) showed that significant amounts of As(III) were retained on different soil constituents, but

around 30% of this were released during desorption tests. Thus, it is reasonable to consider that the environmental impacts caused by As(III) mobility is related to this peculiar desorption behavior rather than to a limited As(III) uptake by the minerals. Therefore, identifying a mechanism that could bring together all experimental observations is still a challenge. In a theoretical approach, Oliveira *et al*. (2006) used density functional methods and cluster models to study two possible processes for the As(III) immobilization on gibbsite: i) the acid/base (ab) mechanism in which H_3AsO_3 behaves like an Arrhenius acid reacting with the base surface of gibbsite; ii) the non-dissociative (nd) mechanism in which the H_3AsO_3 is adsorbed having the OH group bridging the As and Al atomic centers. According to the authors, this non-dissociative mechanism could reconcile the high remobilization of As(III) with the apparently inconsistent formation of inner-sphere adsorption complexes. However, we are not aware of experimental data supporting this proposed mechanism.

Considering the aforementioned context, the present work combines DFT calculations and EXAFS analyses to elucidate the structural environment of As(III) surface complexes on gibbsite, aiming at predicting their stability in Al-rich aqueous environments and, consequently, their potential for remobilization. Various adsorption modes for As(III) linkage on the gibbsite surface were investigated by means of theoretical calculations. Fig. 1 shows the configurations assessed in the present work. The monodentate-mononuclear (mm) complex refers to the configuration in which a single oxygen atom from the arsenite oxyanion coordinates to a single structural aluminum at the Al-hydroxide surface. In a monodentate-binuclear (mb) complex, a single oxygen atom from the arsenite oxyanion is coordinated to two structural Al at the Al-OH surface; in a bidentate-mononuclear (bm) complex, two oxygen atoms from the arsenite oxyanion coordinates a single structural Al at the Al-OH surface; and, finally, in a bidentate-binuclear (bb), two oxygen atoms from the arsenite oxyanion are coordinated to two structural Al atoms at the Al-OH surface. The “ab” and “nd” designations indicate if acid-base or non-dissociative sorption mechanisms were considered. The EXAFS data were collected for As(III) immobilized on gibbsite surface at different pH values (5.0, 7.0 and 9.0) and, as a result, different coverage levels.

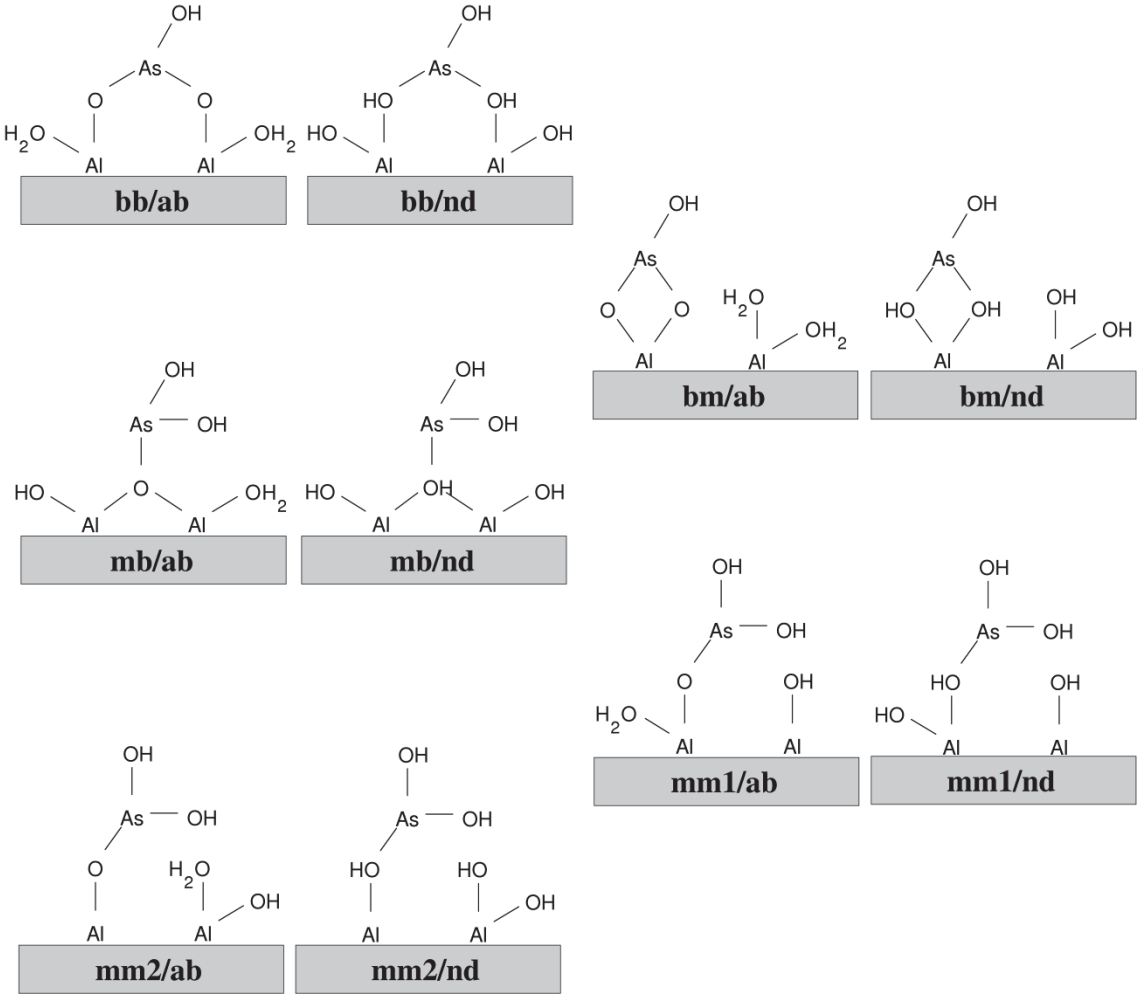

Figure 2.1: Different adsorption complexes of As(III) on gibbsite investigated using the theoretical approach. Nomenclature of the sites: (mm): monodentate-mononuclear, (mb): monodentate-binuclear, (bm): bidentate-mononuclear, (bb): bidentate-binuclear. The “ab” and “nd” designations indicate if acid-base or non-dissociative sorption mechanisms were considered.

2.2 Computational and Experimental Methods

2.2.1 Computational Approach

The adsorption of H_3AsO_3 on gibbsite is particularly challenging for theoretical calculations. Previous investigations by our research group (Oliveira *et al.*, 2006) indicates that many different adsorption sites are available on the gibbsite surface. In this work, monodentate-mononuclear (mm), monodentate-binuclear (mb), bidentate-mononuclear (bm) and bidentate-binuclear (bb) complex configurations were considered for As(III)

sorption on the (010) gibbsite surface, which is representative of all (*hk*0) gibbsite edge surfaces, shown to be more reactive than the (001) basal surface (McBride and Wesselink, 1988). The surface model (see Fig. 2) was derived from the relaxed bulk structure of gibbsite. The bulk structure was relaxed by proportionally varying the cell parameters *a*, *b*, and *c* and performing a full relaxation of the atomic positions until the lowest energy cell was found. In this case, we have obtained *a* = 9.004 Å, *b* = 5.265 Å, and *c* = 10.095 Å, which are 3% larger than the experimental values [Saalfeld and Wedde, 1974]. To build the gibbsite (010) surface model, a periodic slab with approximately 25 Å thickness was cut parallel to the (010) plane of the relaxed gibbsite bulk, resulting in Al-terminated surfaces. Then, each one of the surface Al atoms was saturated by adding a terminal OH group and a coordinated water molecule, in order to restore the octahedral geometry of the Al atoms and neutralize the net electric charge of the model. In addition, a vacuum region of at least 100 Å was added above the slab to ensure that the model does not interact with its own periodic image along the *b* direction. Finally, the slab was replicated once along the *a* direction, to make room for the adsorbates. The final supercell of gibbsite (010) had the following dimensions: *a* = 18.008 Å, *b* = 130 Å (including the vacuum region), *c* = 10.095 Å, and β = 94.54. From this gibbsite (010) model, the adsorption complexes shown in Fig. 1 were constructed by adding one As(III) species below and above the slab, in a total of 554 atoms per model.

The potential energy surface (PES) was explored using the Born-Oppenheimer molecular dynamics (MD) prior to the geometry optimization in order to increase the probability of finding the true global minimum of the potential energy surface. The MD step consisted of linear increase of the temperature up to 320 K in 250 fs, followed by 1000 fs at constant temperature, ending with exponential temperature decrease down to 0 K in 250 fs. The geometry optimization was then performed with the conjugate-gradient algorithm until the maximum force component was lower than 10^{-4} a.u. The potential energy surface (PES) was calculated using the self-consistent charge corrected density-functional based tight-binding (SCC-DFTB) method (Elstner *et al.*, 1998). The PES calculated using the SCC-DFTB was used for performing both MD and geometry optimizations.

The SCC-DFTB method is an approximate density functional theory (DFT) scheme which employs minimal set of atomic basis functions and tight-binding-like approximations. In the DFTB method the three center integrals are neglected and the overlap and two center integrals are previously tabulated and recorded, the so called Slater-Koster files. Then, the secular matrices are easily built, making the calculations much faster. The total energy

has to be corrected due to the approximation made in the hamiltonian by introducing a repulsive potential which is fitted with respect to the DFT calculations used as reference. The self-consistent charge extension of the DFTB method allowed the distribution of charges throughout the molecular structure according to the hardness of the atoms present in the structure. The SCC-DFTB Slater-Koster files used in the present work have been developed in our laboratory (Frenzel et al. 2005) and are available in the deMon-Nano code (Heine et al., 2010), as well as in the DFTB.org website (DFTB, 2010). A recent review of the method can be found elsewhere (Oliveira *et al.*, 2009). The SCC-DFTB has been used successfully to describe gibbsite and aluminosilicate nanotubes (Frenzel et al., 2005; Guimarães *et al.*, 2007). The differences between the SCC-DFTB and DFT calculated structural parameters are not larger than 0.02 Å for Al-Al and Al-O distances. When compared the SCC-DFTB calculated values with the experiment, the differences are not larger than 0.05 Å (Frenzel et al., 2005).

The Γ-point approximation was used for the geometry optimization procedures, while a set of suitable k points was used to sample the irreducible Brillouin zone (IBZ) during the calculation of the final total energies. The k-points were obtained with the Monkhorst-Pack procedure (Monkhorst and Pack, 1976; Pack and Monkhorst, 1977) and a grid of 1×1×2 k points was determined to be enough for the calculation of total energies and assure a convergence within 10^{-3} a.u. All calculations were performed using the DFTB^{+} code (Aradi *et al.*, 2007).

2.2.2 Experimental Approach

2.2.2.1 Materials:

Stock arsenite solution was prepared by dissolving sodium meta-arsenite ($NaAsO_2$ at 99.99% purity - Fluka) in 18MΩ cm Milli-Q water. Synthetic gibbsite was obtained in accordance to Silva et al. (2007), who followed the method proposed by Kyle *et al.* (1975). Other reagents (analytical grade) used in the experiments included sodium arsenate ($Na_2HAsO_4.7H_2O$ at 99% purity - FLUKA), hydrochloric acid (VETEC), and sodium hydroxide (VETEC).

2.2.2.2 Sorption tests:

Sorption tests were carried out batchwise, where 0.3 g of synthetic gibbsite was contacted with 100 mL of As(III) solution (pH 7.0 and initial concentration varying from 0 to 6.5 mmol L^{-1}) into 250 mL Pyrex Erlenmeyer flasks. The vessels were sealed with laboratory parafilm (Pechiney plastic packaging, USA) and stirred at 200 rpm and 25 ± 0.5 ºC using a thermostatic shaker (New Brunswick Scientific Edison, USA). The pH was monitored and if necessary it was adjusted by adding 0.01 mol L^{-1} HCl or NaOH solutions. Ionic strength was fixed at 0.1 by adding NaCl (0.1 mol L^{-1}). After 72 hours, the samples were vacuum-filtered through a 0.45 µm membrane filter (Fisher Scientific). The filtrate was analyzed for total arsenic by flame Atomic Absorption Spectroscopy, AAS (Perkin-Elmer Analyst A300). The filtered solids were rinsed with 50 mL of Milli-Q water, wet-stored in micro-centrifuge tubes (Flex-Tubes®, Eppendorf), and subsequently submitted to spectroscopic analyses. To verify if the sorption mechanism changes with pH, the loading test for the highest initial concentration sample was repeated at pH 5.0 and 9.0. All the sorption tests were carried out in duplicate.

2.2.2.3 XAFS analyses:

X-ray absorption near edge structure (XANES) and extended X-ray absorption fine structure (EXAFS) analyses of the gibbsite samples loaded with As(III) were performed using the synchrotron facilities at the *Laboratório Nacional de Luz Síncrotron* (LNLS), in Campinas, Brazil. XANES and EXAFS data of the arsenic K edge (11868 eV) were obtained at XAFS2 workstation in the fluorescence mode, under operation conditions of 1.37 GeV and beam currents of approximately 250 mA. The spectra were collected at room temperature using a Si (111) double crystal monochromator with an upstream vertical aperture of 0.3 mm and calibrated with Au L_1-edge (11918 eV). The samples were fixed onto acrylic holders, sealed with Kapton tape film, placed at an angle of 40° to the incident beam, and the signal was monitored using a 15-element Ge detector (Canberra Industries). Energy calibration was monitored during data collection by acquiring reference Au foil spectra simultaneously. The obtained data were analyzed as described in Vasconcelos *et al*. (2008) by using the Athena and Artemis software from the IFEFFIT computer package (Ravel and Newville, 2005). Firstly, the data were processed in Athena, where several scans from the same sample were aligned by the reference spectra and merged in energy space. Edge energy value, E_0, was chosen at the inflection

point of the absorption edge. Next, the pre-edge and post-edge backgrounds were removed and the spectra normalized to a step height of 1. The isolated EXAFS oscillations were converted from energy (χ(E) data) to wavenumber space (χ(k) data) and Fourier Transformed. The Fourier-transformed data were fitted using the Artemis software. Theoretical phase shift and scattering amplitude parameters were calculated by means of FEFF 6.0 code included in the IFFEFIT package (Ravel and Newville, 2005). Fits to all samples were performed using a simultaneous k-weighting of 1, 2 and 3 to decrease the possibility that correlations between fitting parameters could compensate for a misfit in a particular k-weighting. The passive electron reduction factor (S_0^2) obtained from fit to a crystalline standard (As_2O_3) was 0.95 ± 0.08 for the As K-edge. This value was used in all fits to the data.

2.3 Results

2.3.1 SCC-DFTB calculations of As(III) adsorption on gibbsite

Different adsorption sites have been investigated using the slab model of the surface as shown in Figure 2.1. In order to allow a direct comparison of the different adsorption complexes, H_2O or –OH groups were added to keep their charge neutrality and the coordination number of the Al centers. The results for the most favorable adsorption sites are shown in Table 2.1. All the other adsorption sites are at least 50 kcal mol^{-1} higher in energy and will not be discussed here.

Table 2.1: Relative energies and structural parameters of the most favorable adsorption complexes.

Adsorption complex	ΔE (kcal.mol^{-1})	As-Al distance (Å)	As-O distance (Å)
bb/ab	0.0	3.24	1.75
mm/ab	11.2	3.29	1.85
mm/nd	33.3	3.38	1.80
bb/nd	51.0	3.12	1.82
mb/ab	90.5	3.47	1.80

Regarding the solvent effects, there is a consensus in the literature (Kubicki *et al.*, 2007; Hatorri *et al*., 2009) that placing water molecules in the empty coordination sites of the metal centers is crucial to permit a reasonable description of the thermodynamics of the system and, consequently, the chemical speciation. Indeed, it has been the subject of many studies in our group (Rodrigues *et al.*, 2010; Abreu *et al.*, 2008; Noronha *et al*, 2007; Guimarães *et al*., 2007; Abreu *et al*., 2006). However, in the case of the arsenous acid, at the pH range used at the experiments, the predominant species is fully protonated H_3AsO_3, (pKa ~9). The process of adsorption may thus follow the two mechanisms suggested by Oliveira *et al.* (2006). It can be asked if water molecules surrounding the H_3AsO_3 forming hydrogen bonds are not necessary. In Oliveira *et al.* (2006) this possibility is discussed in detail. In summary, it is reasonable to expect that the solvation energy of the surface occupied by the H_3AsO_3 is similar to the solvation energy of the H_3AsO_3 itself, leading to a cancelation of errors. Furthermore, the present study is more interested in obtaining accurate geometries and relative energies of the different adsorption sites, and the solvent effects do not seem to change drastically the relative stability of the complexes evaluated in this work.

The structural parameters are known to be a local property, therefore the model used is adequate and reliable. The most difficult part is to assure that the potential energy surface has been explored enough to find the most favorable adsorption site. Using the approximate DFT method, larger models can be used to investigate a larger number of possible sites, thus making the method particularly interesting to the present investigation. Therefore, the molecular dynamic simulation has been used together with the SCC-DFTB to explore the vicinities of each adsorption mode described in Fig.1. The binuclear-bidentate/acid-base adsorption (bb/ab) shown in Fig. 2 was found to be the most stable complex for As(III) adsorption on gibbsite surface with As-Al and As-O distances of 3.24 and 1.70 Å, respectively. These values are in good agreement with the DFT calculations on small cluster models performed by Oliveira *et al.* (2006), who obtained 3.21 Å for the As-Al distance in the bb/ab adsorption complex.

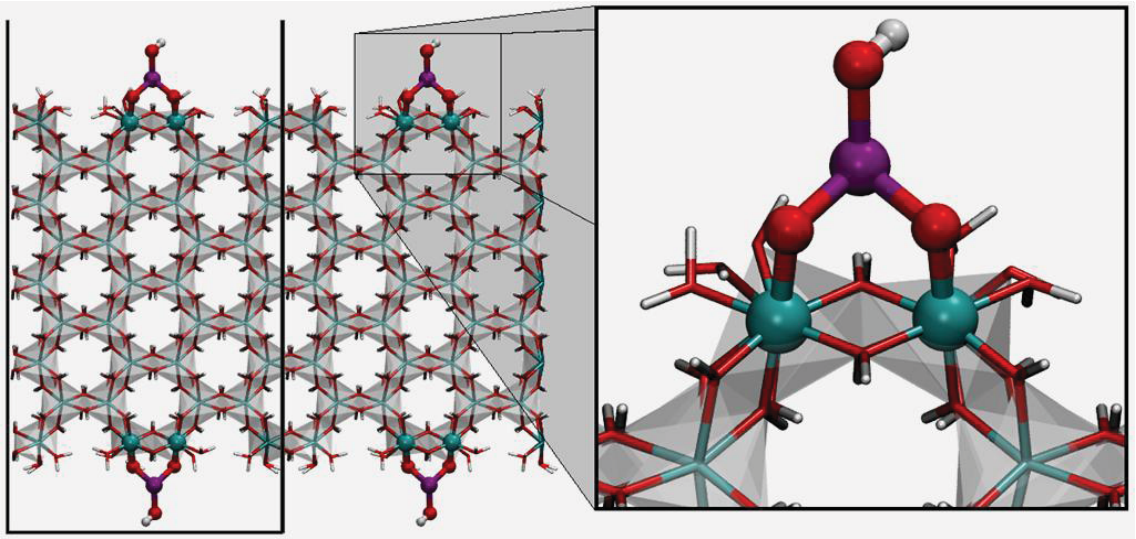

Figure 2.2: Perspective view of the bb/ab adsorption complex in the edge of the gibbsite.

2.3.2 XAFS analyses of As(III) adsorption on gibbsite

Figure 2.3 shows the isotherm obtained for As(III) sorption on gibbsite at pH 7.0, where the highest coverage level was found to be equal to 0.0054 $mmol_{As(III)}$ m^{-2}. This sorption experiment was repeated at pH 5 and 9, and it was found that the maximum loading was lower at pH 5.0 (0.0024 $mol_{As(III)}$ m^{-2}) than at pH 7. At pH 9.0 the loading was equal to 0.0058 $mmol_{As(III)}.m^{-2}$, which is similar to the value found at pH 7. The samples showing the highest coverage levels at each selected pH were used for XAFS measurements, and they are summarized in Table 2.2.

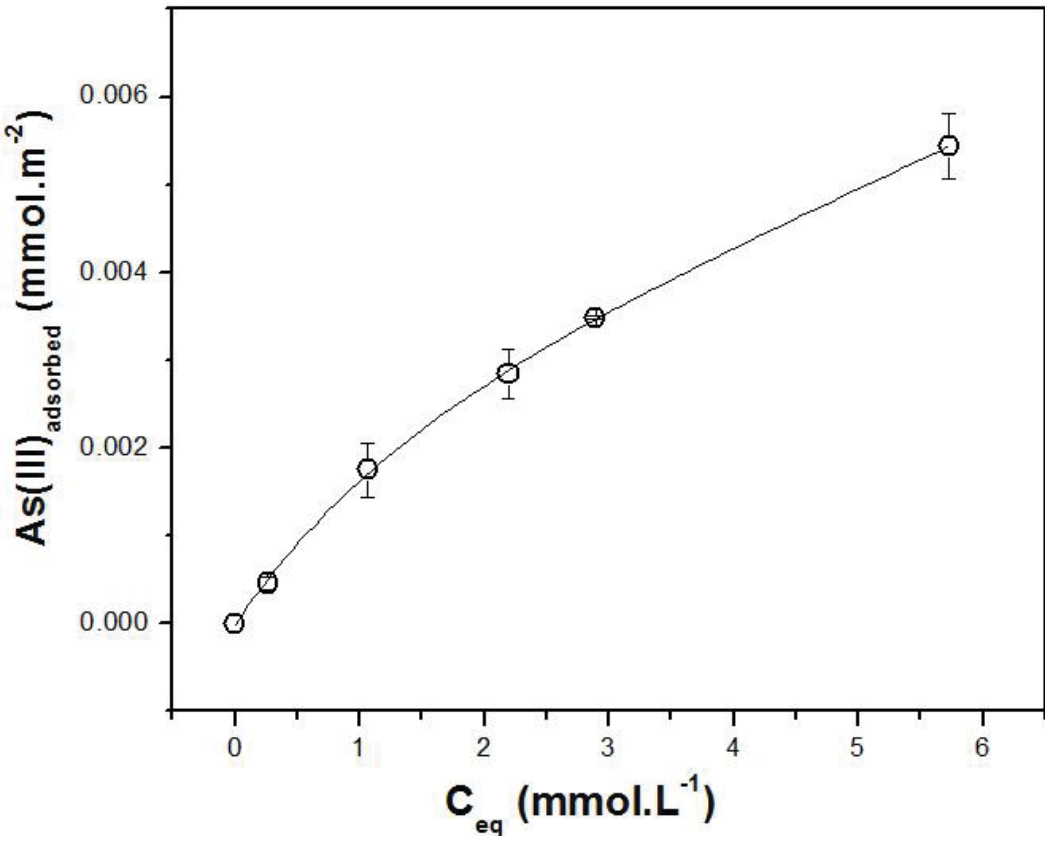

Figure 2.3: Isotherm for As(III) adsorption on gibbsite at pH 7.0, 25 °C, 200 rpm, ionic strength of 0.1, and S/L ratio of 3 g L^{-1}. Sorption tests were carried out in duplicates.

Table 2.2: List of samples used for XAFS analyses.

Samples	pH	$[As]_{adsorbed}$ ($mmol.m^{-2}$)
I	5.0	0.0025
II	7.0	0.0054
III	9.0	0.0058

Figure 2.4 compares the normalized As K-edge XANES spectra of evaluated samples and standards. Fig. 4 (b), (c) and (d) show the derivative As K-edge XANES spectra for the As(III)-Gibbsite sorbed at pH 9.0, 7.0, and 5.0, respectively, compared to the solution and solids standards. As can be seen, the derivative spectra for the As(III)-Gibbsite samples overlaps the derivative spectra of the $NaAsO_2$ standard at all pH assessed. This indicates that As(III) was not oxidized, at least not significantly, to As(V) during the sorption process. The possibility of As(III) oxidation by the beamline was also checked and it was not verified the occurrence of such process.

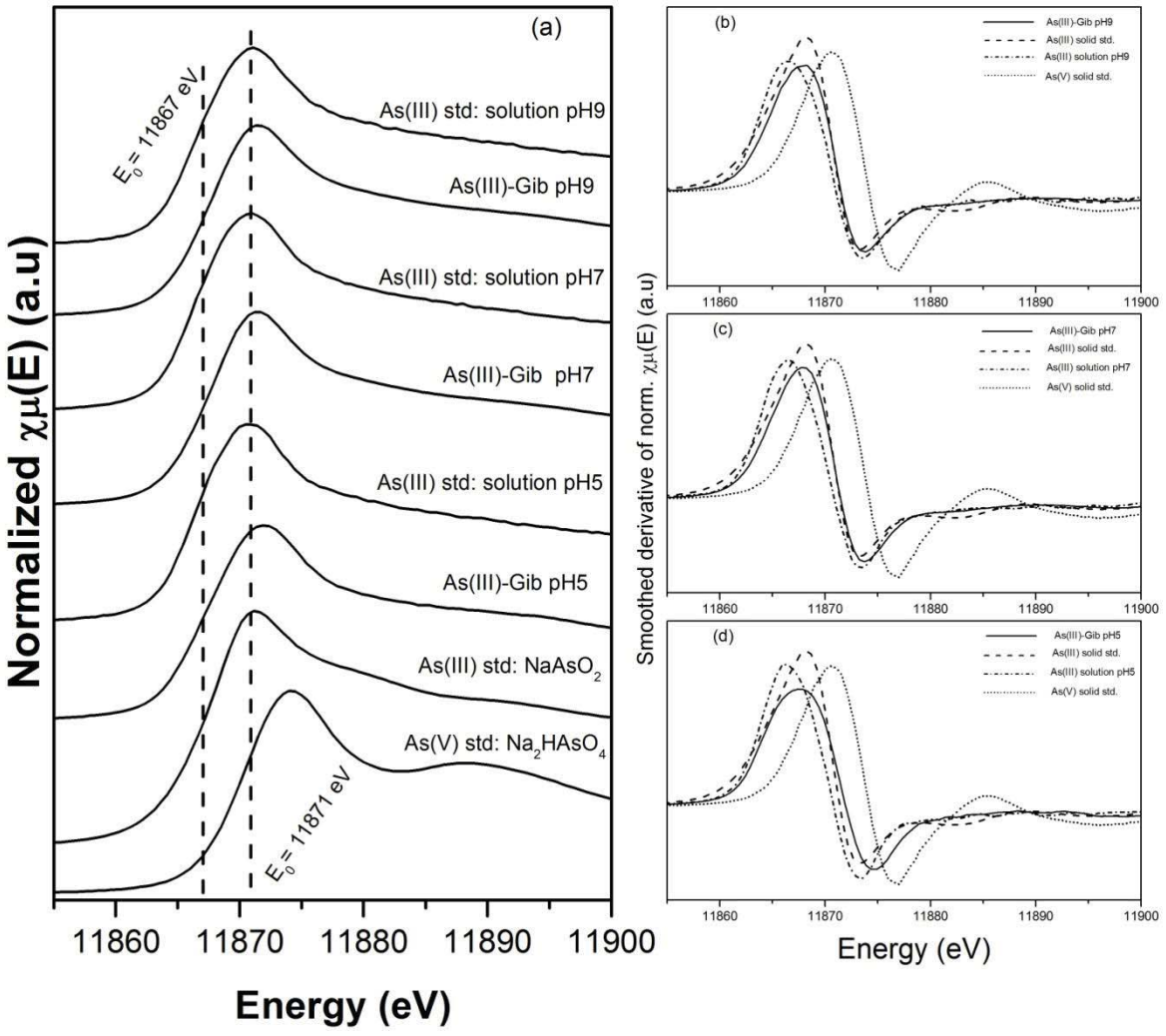

Figure 2.4: (a) Normalized As K-edge XANES spectra of As(III)-loaded gibbsite, As(III) solutions at pH 5.0, 7.0, and 9.0; and $NaAsO_2$ and $Na_2HAsO_4.7H_2O$ solid standards; (b) (c) and (d): Smoothed derivative of the normalized As K-edge XANES spectra for As(III)-loaded gibbsite and As(III) solution at pH 9.0, 7.0, and 5.0, respectively, besides $NaAsO_2$ and $Na_2HAsO_4.7H_2O$ solid standards.

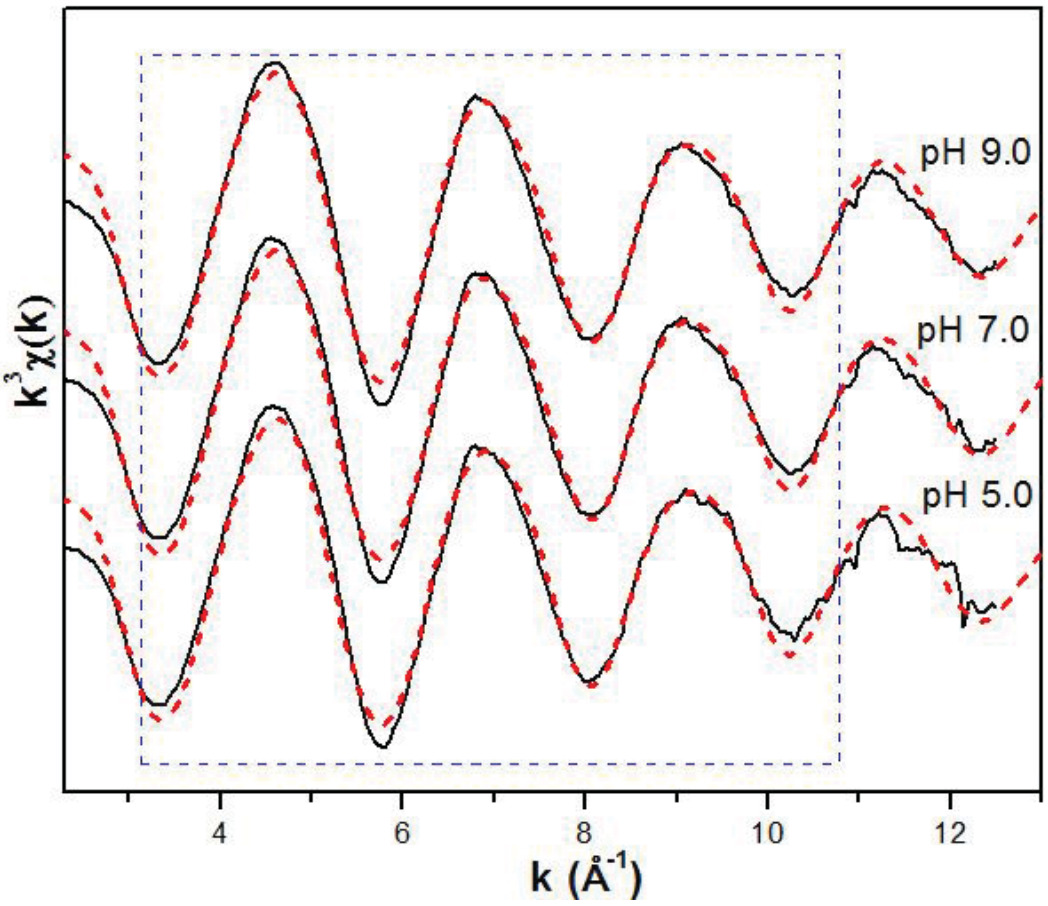

Figure 2.5: k^3- weighted $\chi(k)$ data for As(III) on gibbsite at different pH values. Window shows the k-range used in all fits to the data.

To investigate the local structure of arsenic on gibbsite, the Fourier-transformed EXAFS spectrum was fitted using As-O and As-Al scattering paths derived from the structures of sodium meta-arsenite ($NaAsO_2$), mansfieldite ($AlAsO_4.2H_2O$) and Al-substituted tooeleite ($Al_6(AsO_3)_4SO_4(OH)_4{\cdot}4H_2O$). These paths were obtained from FEFF 6.0 code built-in the Artemis software (Ravel and Newville, 2005). The three datasets assessed were fit simultaneously (R range from 1.0 to 3.5 Å) with a single ΔE_0 value. This method is useful when a similar model is applied to fit a series of samples. Besides, fitting datasets simultaneously increases the number of independent data points, which decreases errors associated with the fitting parameters and decreases correlations between variables, increasing then the confidence in the final fitted values. During the fitting, the coordination number (N) for the As-Al interaction was set at 1 or 2, which designate different fit models. The fit with the N set at 1 considered the occurrence of mm or bm complex types, where a single or two oxygen atoms from the arsenite oxyanion are coordinated to a single aluminum at the Al-hydroxide surface. The N set at 2 could indicate the occurrence of bb or mb complex configurations, in which a single or two oxygen atoms from the arsenite oxyanion, respectively, are coordinated to two Al at the Al-OH surface. Figure 2.6 (a) shows the real part of the Fourier-transformed EXAFS region of the As K-edge XAFS spectra for the gibbsite loaded with As(III) at different pH values, together with the best fitting curve for each sample. The individual contributions of the As-O, and As-Al scattering paths to the fits of the sample at pH 7.0 are shown in Figure 2.6 (b). Due to similarities with the pH 7 sample, the other two samples (pH 5 and pH 9) are not repeated in Figure 2.6 (b). However, they were fitted using the same scattering paths shown for pH 7. Figure 2.7 shows the magnitude EXAFS spectra of the samples at the evaluated pH. The best fits to EXAFS data are summarized in Table 2.3.

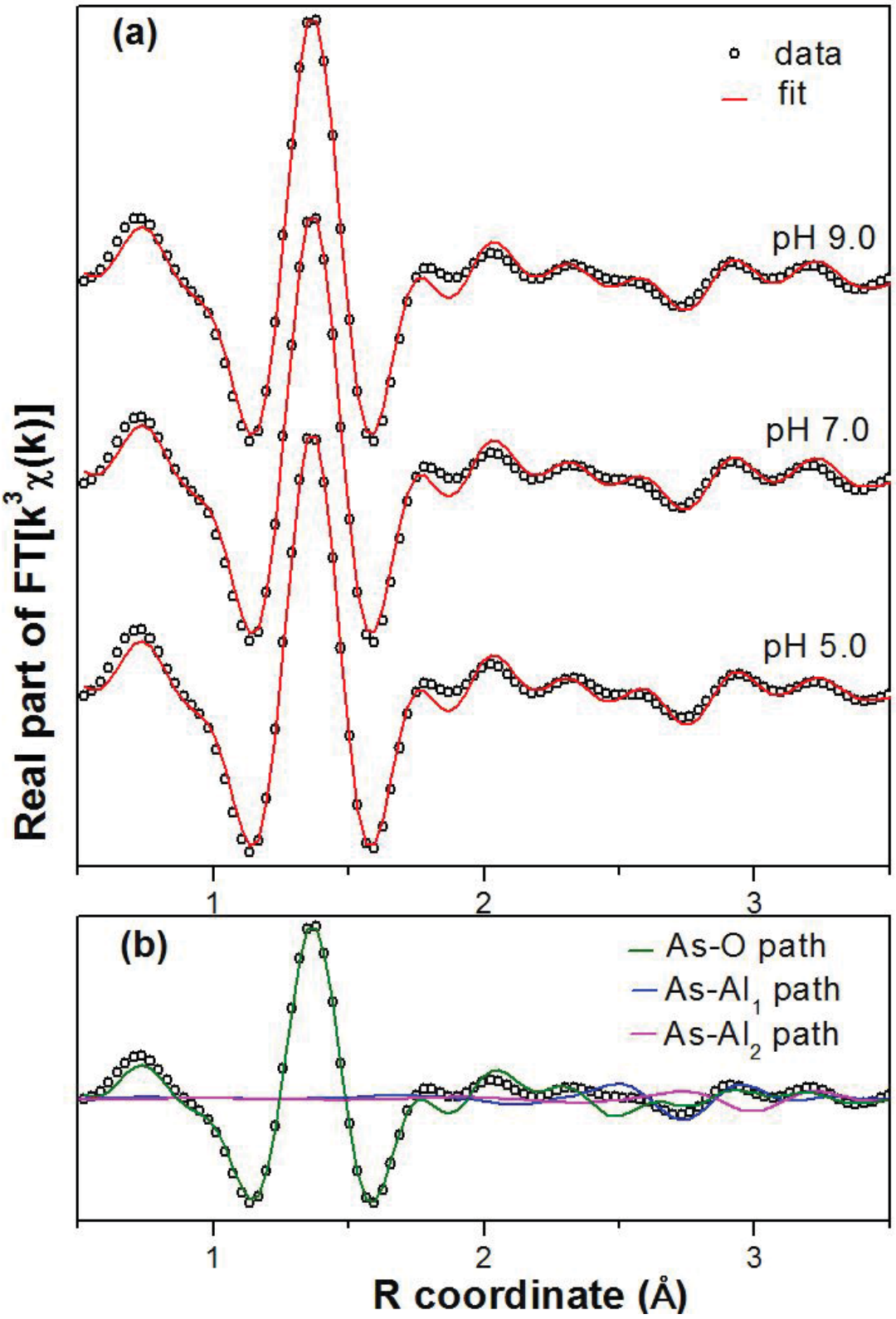

Figure 2.6: Real part of the Fourier-transformed As K-edge EXAFS data for (a) As(III)-loaded gibbsite at different pH values - scatter and line curves represent data and fit, respectively; and (b) individual contributions of scattering paths used to the fits.

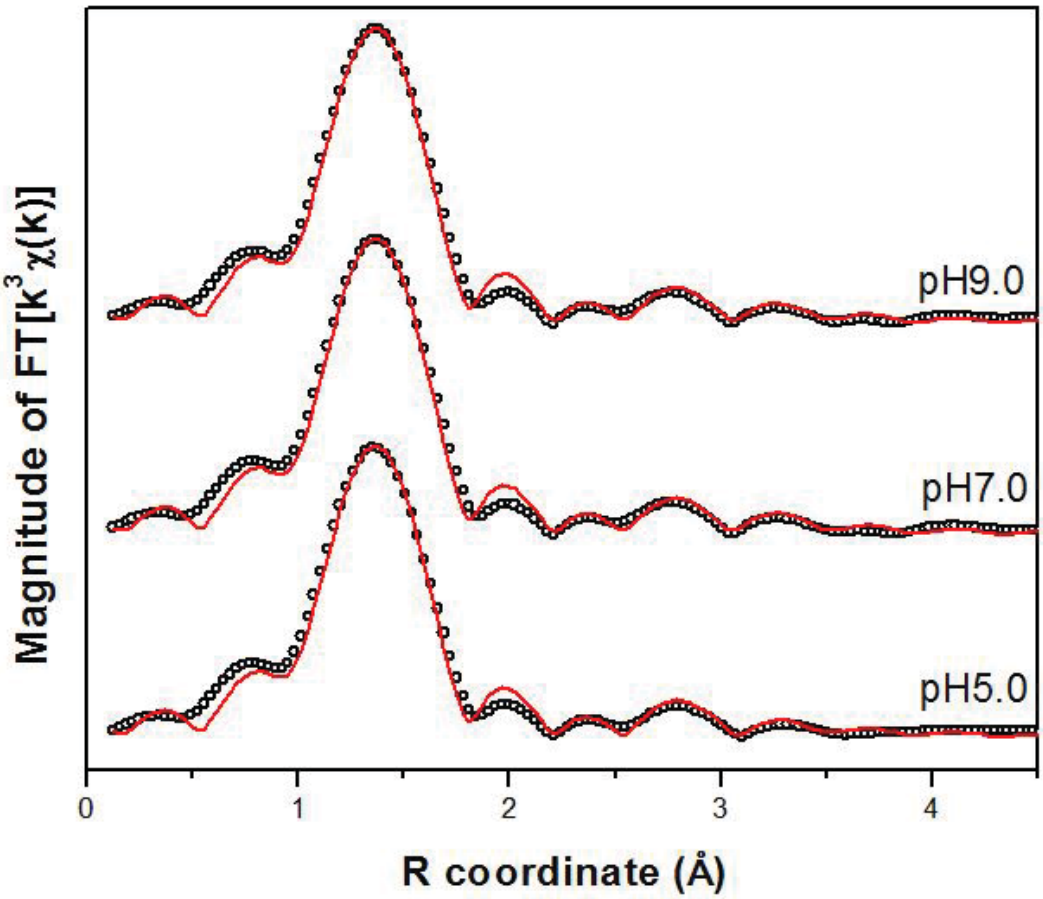

Figure 2.7: Magnitude of the Fourier-transformed As K-edge EXAFS data for (a) As(III)-loaded gibbsite at different pH values - scatter and line curves represent data and fit, respectively.

Table 2.3: Results of fits to EXAFS data.

Samples	As-O			As-Al_1			As-Al_2			ΔE_0	
	N	R (Å)	σ^2 (Å^2)	N*	R (Å)	σ^2 (Å^2)	N*	R (Å)	σ^2 (Å^2)	(eV)	χ^2 Red.
I (pH 5)	3.4± 0.2	1.771± 0.004	0.005± 0.001	2	3.21± 0.03	0.011± 0.005	2	3.49± 0.06	0.019± 0.011	11.1± 0.7	54.2
							1	3.49± 0.07	0.011± 0.009	11.1± 0.7	57.4
				1	3.18± 0.04	0.006± 0.004	2	3.43± 0.07	0.023± 0.015	11.0± 0.7	57.8
							1	3.43± 0.09	0.014± 0.014	10.9± 0.8	62.5
II (pH 7)	3.4± 0.2	1.773± 0.004	0.004± 0.001	2	3.20± 0.03	0.010± 0.004	2	3.47± 0.04	0.014± 0.006	11.1± 0.7	54.2
							1	3.47± 0.04	0.007± 0.005	11.1± 0.7	57.4
				1	3.18± 0.03	0.005± 0.003	2	3.43± 0.06	0.019± 0.009	11.0± 0.7	57.8
							1	3.42± 0.06	0.010± 0.008	10.9± 0.8	62.5
III (pH 9)	3.4± 0.2	1.773± 0.004	0.005± 0.001	2	3.20± 0.03	0.011± 0.004	2	3.47± 0.05	0.016± 0.007	11.1± 0.7	54.2
							1	3.47± 0.05	0.008± 0.005	11.1± 0.7	57.4
				1	3.18± 0.03	0.006± 0.004	2	3.42± 0.06	0.019± 0.010	11.0± 0.7	57.8
							1	3.42± 0.06	0.011± 0.008	10.9± 0.8	62.5

R = Interatomic distance;

N = Coordination number;

σ^2 = Debye–Waller factor;

ΔE_0 = difference between the user-defined and the experimentally determined threshold energy;

* *Fixed parameter;*

** *Considering N $_{AsAl1}$ = 2*

*** *All samples were fitted using the same ΔE_0 for each fitting condition.*

Results shown in Table 3 indicate that at pH 7.0 the arsenic atom is coordinated by 3.3 ± 0.2 oxygen atoms at a distance of 1.77 ± 0.01 Å in the first shell. The coordination number of 3 oxygen atoms in the first coordination shell is in agreement with the expected pyramidal geometry of the As(III) species, H_3AsO_3, predominant in solution at pH < 9.0. Regarding the second shell, firstly only the As-Al_1 path (from mansfieldite structure) contribution to the fitting was considered, with coordination number (N) set at 1 or 2. At pH 7.0, the fitting returned an As-Al_1 distance of 3.20 ± 0.03 Å for N = 2, and an As-Al_1 distance of 3.18 ± 0.03 for N = 1. Thus, it is reasonable to say that the As-Al distances are very similar (around 3.2 Å), independent of the coordination number considered in the fitting. This observation gives the confidence that the As-Al distance in the second shell is in fact around 3.2 Å. It is known from literature that the typical interatomic distance for As-Al and As-Fe interactions when arsenic is sorbed on Al and Fe oxy-hydroxides at bidentate-binuclear configuration is approximately 3.2 Å (Ladeira *et al*., 2001; Arai *et al.*, 2001; Sherman and Randal, 2003). Therefore, the As-Al distance from our EXAFS results is in agreement with the literature, indicating the occurrence of bidentate-binuclear complexation of As(III) on gibbsite at the conditions evaluated in the present work.

With respect to the more dilute samples, it was found that at pH 7.0 the As(III) is coordinated to 3.1 ± 0.3 oxygen atoms at a distance of 1.77 ± 0.01 Å in the first shell; to aluminum at a distance of 3.23±0.06 Å, and to another Al atom at a distance of 3.5 ± 0.1 Å. The number of independent points and variables in this case were 55.4 and 29, respectively (χ^2 – reduced = 43.9 and R-factor = 1%).

Regarding the pH effects on the As(III) complexation on gibbsite, the As-O and As-Al interatomic distances remained virtually unchanged regardless of the value of pH evaluated (Table 2.3). This suggests that, although the As(III) loading increases with increasing pH from 5 to 9, its sorption mechanism on gibbsite is not significantly dependent on the pH, under the conditions of the present investigation.

During the fitting to EXAFS data, the contribution of another As-Al interaction in the system became apparent, and thus an As-Al_2 path (from Al-substituted tooeleite structure) was added to the model. The As-Al_2 path was considered using different coordination numbers (set at 1 and 2), and all of them have returned similar As-Al interatomic distances (~3.49 Å). By comparing the As-Al experimental distance (3.48 ± 0.06 Å) to the results from theoretical calculations shown in Table 2.1, it is possible to verify that the value is close to the monodentate-binuclear (mb) configuration. To elucidate the

improvement in the fit to the data when considering a second As-Al path in the model, the fit in the range 2.3-3.5 Å was carried out in the presence and absence of this As-Al_2 path. As can be seen in Figure 2.8, the addition of the As-Al_2 path in the model improves the fit. In fact, the χ^2-reduced factor decreased from 35 to 24 and the relative misfit (R-factor) decreases from 12% to 5% in the range of 2.3-3.5 Å.

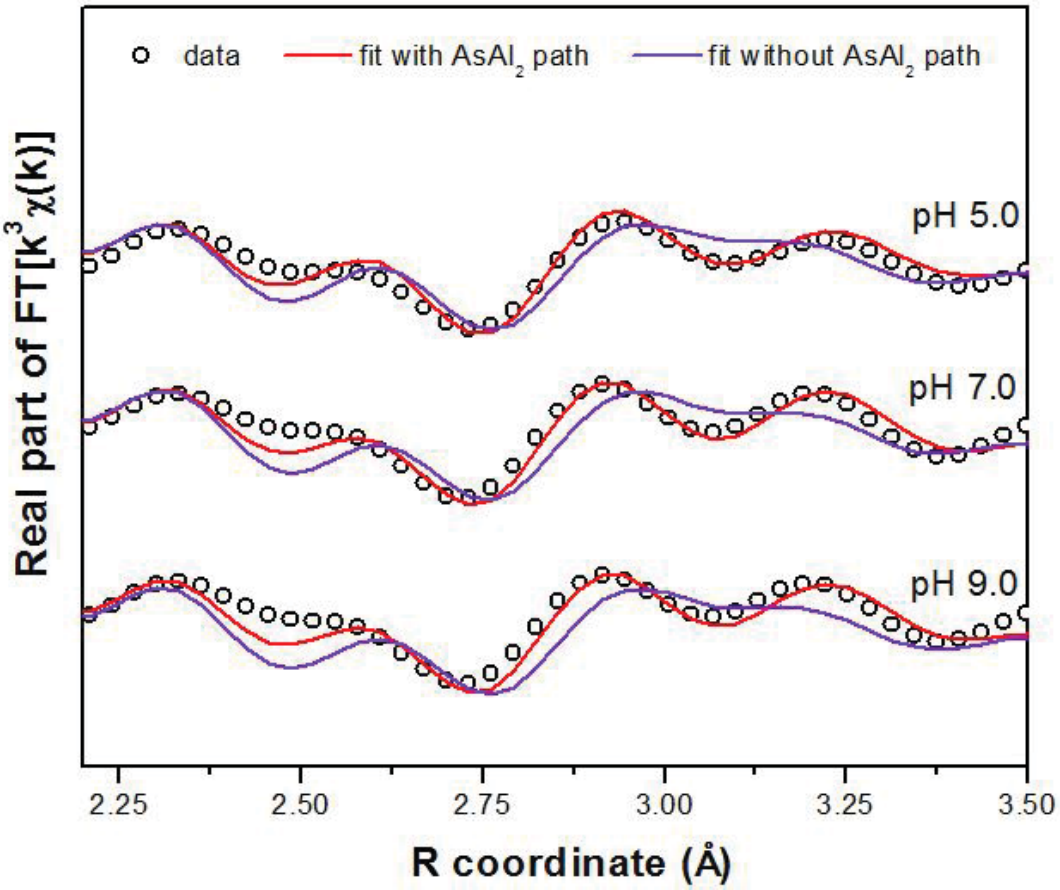

Figure 2.8: Real part of the Fourier-transformed As K-edge EXAFS data in the range 2.3-3.5 Å for As(III)-loaded gibbsite at different pH values. Scatter and line curves represent data and fit, respectively.

2.4 Discussion

Comparing the theoretical and experimental results, it is observed a convergence between the optimized geometry and the obtained geometrical EXAFS parameters. SCC-DFTB calculations indicated the bidentate-binuclear complex (bb/ab) to be the most favorable geometry for As(III) linkage on gibbsite surface with As-O and As-Al distances of 1.75 and 3.24 Å, respectively. EXAFS results found that arsenic is coordinated to 3 oxygen atoms at a distance of 1.77 Å in the first shell, and bonded to aluminum at a distance around 3.2 Å regardless of the coordination number considered for the second shell (1 or 2) and the pH assessed (5, 7 and 9). This As-Al distance of 3.2 Å is found in the literature to be typical of inner-sphere bidentate-binuclear complexation of arsenic on Al and Fe oxides and oxy-hydroxides (Ladeira et al., 2001; Arai et al., 2001; Sherman and Randal, 2003). Thus, EXAFS results and theoretical estimates provide evidences that, amongst the evaluated geometries, inner-sphere bidentate binuclear complexation is the preferable configuration for the As(III) on gibbsite surface. It is important to highlight that the fits to EXAFS data were not based on DFT results, and that these modeling techniques were performed in a completely independent manner. The good agreement between these independent approaches supports the conclusions of the present work.

One may argue about the method used to fit the EXAFS data by setting an important parameter as the coordination number. It is important to make clear that the authors are aware of the limitations of such approach. However, the proposition of the inner-sphere bidentate-binuclear complexation as the preferable configuration for the evaluated system has been based on the observed interatomic As-Al distance, and not in the coordination number, which was fixed for the second shell during the fit. Furthermore, considering that the system under study in this work is not a well-ordered one, and the quality of the data is unavoidably limited by operating conditions, it is suitable to use the alternative of setting parameters to reach an accurate fitting. Indeed, this approach of constraining some parameters during EXAFS fitting is usually found in the literature (Arai *et al*., 2001; Sherman and Randal, 2003; Bostick and Fendorf, 2003; Arai *et al*., 2004; Paktunc *et al.*, 2008; Chen *et al*., 2009; Voegelin *et al*., 2010). Some of these mentioned investigations have set the coordination numbers (Bostick and Fendorf, 2003; Paktunc *et al.*, 2008; Chen et al., 2009; Voegelin *et al*., 2010) while others have fixed the Debye-Waller factor (Arai *et al*., 2001; Sherman and Randal, 2003; Arai *et al*., 2004) for the second shell fitting. In this work, it was chosen to set the coordination number instead of the Debye-Waller factor because of previous indication from theoretical calculations regarding the possible

coordination numbers for the As(III)-gibbsite system. As shown in section 3.1, the most thermodynamically favorable configurations for the As-Al interaction would present coordination numbers of 2 or 1. These values are also supported by the results obtained in similar systems (Arai *et al*., 2001; Ladeira *et. al*., 2001; Sherman and Randal, 2003) and A

Regarding the contribution of the As-Al_2 interaction in the system, the improvement in the fitting quality was evidenced when considering this path in the model (Figure 2.8). One may argue about the relatively high energy of the mb/ab sorption complex used to fit the As-Al_2 contribution in the EXAFS spectra, when compared to the other configurations evaluated during theoretical calculations. However, larger distances generally mean weakly bound complexes, as suggested by the mb/ab-calculated As-Al distance of 3.47 Å. Therefore, other effects such as ionic strength, pH and solvation might be important to be considered in order to accurately simulate the thermodynamics (e.g. energy) of the system. The relative stability of the different adsorption sites may be easily modified upon consideration of these effects. However, the geometry (e.g. distances) of these sites is not expected to be significantly altered by these effects, since adsorption is a local phenomenon. The EXAFS estimated As-Al_2 distance of 3.49 Å is in good agreement with the mb/ab adsorption site as shown in Table 2.3, and the As-O distance of 1.77 Å is about 0.03 Å lower than the calculated value. These results indicate that the mb/ab adsorption site may be assigned as the adsorption site observed in the As-Al_2 path proposed in the EXAFS analyses, despite its relatively high energy.

Considering the literature regarding As(III) interactions on gibbsite, Weerasooriya *et al*. (2003) proposed that As(III) forms an outer-sphere surface complex with gibbsite. These authors based their suggestion on indirect macroscopic evidences of sorption dependency with pH and ionic strength. Goldberg and Johnston (2001) also suggested that As(III) forms outer-sphere complexes on amorphous $Al(OH)_3$ considering their results from Based on Raman and FTIR spectroscopy, sorption, and electrophoretic mobility measurements. Arai *et al* (2001) used XAFS analyses to propose a mechanism for As(III) sorption on alumina (γ-Al_2O_3) at pH 5.5 and 8.0. The results for As-O (1.75 to 1.78Å) and As-Al (3.19 to 3.22Å) interatomic distances are similar to the As-O (1.77Å) and As-Al_1 (3.21Å) values obtained in the present work. These authors suggested that As(III) forms a bidentate-binuclear complex on alumina surface at pH 5.5, regardless of the ionic strength (*IS*). At pH 8.0, a mixture of inner- and outer-sphere As(III) complexes would coexist, with outer-sphere complexes becoming more important as ionic strength decreases. These

authors based their hypothesis of a change in the sorption mechanism on XANES analyses. According to them, the spectrum of the sample reacted at pH 8 and *IS* = 0.01 mol L^{-1} appeared to be intermediate between the aqueous As(III) spectrum and the spectra of the other As(III) adsorption samples. It was then suggested that this apparent difference indicated a mixture of inner-sphere and outer-sphere As(III) complexes at pH 8. In the present work, no significant alterations in XANES spectra of As(III) immobilized on gibbsite were found as pH increased from 5 to 9 (Figure 2.4).

In summary, the present work demonstrates the formation of inner-sphere bidentate-binuclear complexes during As(III) sorption on gibbsite surface according to both theoretical and experimental techniques. It should be clarified that the formation of outer-sphere complexes cannot be disregarded. However, it is clear from our DFT and EXAFS results that inner-sphere complexation of As(III) occurs on gibbsite, a fact that has not been widely recognized yet in the literature.

Regarding the practical implications of the results obtained in the present work, one may consider the often-stated argument that the As(III) mobility in the environment is higher than the As(V) mobility due to the neutral character of the arsenite molecule in a wide pH range (< 9.2) as too simplistic. Like As(V) (Ladeira *et al*.,2001), As(III) was also demonstrated to form inner-sphere complexes on gibbsite's surface in a pH interval (pH 5 to 9) where the neutral H_3AsO_3 predominates. In order to understand such higher mobility of the As(III) it is important to notice the following: the first pK_a of H_3AsO_3 is about 9.2, and the point of zero charge (pzc) of gibbsite and other aluminum oxides is in the pH range of 8-10 (Ladeira and Ciminelli, 2004; Arai *et al*., 2001; Goldberg and Johnston, 2001). It means that the gibbsite surface has similar ability to accept protons as the As(III) sorbed complex. Therefore, it is proposed that the higher As(III) mobility in the environment is related to the feasibility of protonation of the inner-sphere As(III) complexes, besides the protonation of the Al oxyhydroxides surfaces. This protonation would restore the neutral H_3AsO_3 molecule, which could be released from the mineral surface, as it has already been discussed by Oliveira *et al.* (2006).

2.5 Conclusions

The results from theoretical calculations combined with EXAFS analyses obtained in this work indicate that inner-sphere complexation is a feasible mechanism for arsenite adsorption on gibbsite at pH varying from 5 to 9. Several adsorption sites have been evaluated using SCC-DFTB calculations and the most stable structure predicted for the As(III)-gibbsite system is the bidentate-binuclear configuration. EXAFS results also indicated that As(III) forms inner-sphere complexes on gibbsite. It was shown that the arsenic coordinated to three oxygen atoms in the first shell, at a distance of 1.77 Å, and to aluminum in the second shell at a distance of approximately 3.20 Å, typical of bidentate-binuclear configuration, for all evaluated pH values (5.0, 7.0 and 9.0). In addition, an As-Al_2 interaction, ascribed to the monodentate-binuclear complex because of its interatomic distance of 3.47 Å, was shown from EXAFS results to contribute to As(III) sorption on gibbsite, considering the conditions used in this work. Based on these results, it was proposed that the higher As(III) mobility in the environment, when compared to As(V), may be related to the protonation of the As(III) inner-sphere complexes formed on the mineral surface. Such protonation would restore the neutral H_3AsO_3 molecule, which could be easily released to aqueous environments. The understanding of As(III) interactions with gibbsite is pointed out as an important outcome from this work, considering the relevance in predicting and controlling arsenic mobility in natural environments, where gibbsite is often found.

2.6 References

ABREU, H. A.; GUIMARÃES, L., and DUARTE, H. A. (2008). DFT/PCM investigation of the Mn(II) chemical speciation in aqueous solution. *International Journal of Quantum Chemistry* vol. 108, 2467 - 2475.

ABREU, H. A.; GUIMARÃES, L., and DUARTE, H. A. (2006). Density-Functional Theory study of iron(III) hydrolysis in aqueous solution. *Journal of Physical Chemistry A* vol. 110 (24), 7713 - 7718.

ARADI B., HOURAHINE B., and FRAUENHEIM T. (2007). DFTB+, a Sparse matrix-based implementation of the DFTB method. *Journal of Physical Chemistry A,* vol. 111, 5678 – 5684

ARAI Y., ELZINGA E. and SPARKS D. L. (2001). X-ray absorption spectroscopic investigation of arsenite and arsenate adsorption at the aluminum oxide–water interface. *Journal of Colloid Interface Science,* vol. 235, 80 - 88.

ARAI Y., SPARKS D. L., and DAVIS J. A. (2004). Effects of dissolved carbonate on arsenate adsorption and surface speciation at the hematite-water interface. *Environmental Science & Technology* vol. 38 (3), 817 - 824.

BOSTICK B C., and FENDORF S. (2003). Arsenite sorption on troilite (FeS) and pyrite (FeS_2). *Geochimica et Cosmochimica Acta* vol. 67 (5), 909 - 921.

CHEN N., JIANG D.T., CUTLER J., KOTZER T., JIA Y.F., DEMOPOULOS G.P., ROWSON J.W. (2009). Structural characterization of poorly-crystalline scorodite, iron(III)–arsenate co-precipitates and uranium mill neutralized raffinate solids using X-ray absorption fine structure spectroscopy. *Geochimica et Cosmochimica* Acta vol. 73 3260 - 3276.

DFTB web site: http://www.dftb.org. Accessed: August 12th 2010.

DIXIT S. and HERING J. G. (2003). Comparison of arsenic(V) and arsenic(III) sorption onto iron oxide minerals: implications for arsenic mobility. *Environmental Science and Technology* vol. 37, 4182 - 4189.

ELSTNER M., POREZAG D., JUNGNICKEL G., ELSNER J., HAUGK M., FRAUENHEIM T., SUHAI S. and SEIFERT G. (1998). Self-consistent-charge density-functional tight-binding method for simulations of complex materials properties. *Physical Review B,* vol. 58, 7260 - 7268.

FENDORF S., EICK M.J., GROSSL P. and SPARKS D.L. (1997). Arsenate and chromate retention mechanisms on goethite. 1. Surface structure. *Environmental Science and Technology,* vol. 31 (2) 315 - 320.

FRENZEL J., OLIVEIRA A. F., DUARTE H. A, HEINE T., and SEIFERT G. (2005). Structural and electronic properties of bulk gibbsite and gibbsite surfaces, *Zeitschrift für anorganische und allgemeine Chemie (ZAAC),* vol. 631, 1267-1271.

GOLDBERG S. and JOHNSTON C.T. (2001). Mechanisms of arsenic adsorption on amorphous oxides evaluated using macroscopic measurements, vibrational spectroscopy, and surface complexation modeling. *Journal of Colloid Interface Science,* vol. 234, 204 - 216.

GUIMARÃES L, ENYASHIN A N., FRENZEL J., HEINE T., DUARTE H A. and SEIFERT G. (2007). Imogolite nanotubes: stability, electronic and mechanical propertie., *ACS Nano 2007,* vol. 1, 362 - 368.

GUIMARÃES, L.; ABREU, H. A. and DUARTE, H. A. (2007). Fe(II) hydrolysis in aqueous solution: A DFT study. *Chemical Physics,* vol. 333, 10 - 17.

HATTORI, T.; SAITO, T.; ISHIDA, K.; SCHEINOST, A. C.; TSUNEDA, T.; NAGASAKI S.; TANAKA, S. The structure of monomeric and dimeric uranyl adsorption complexes on gibbsite: A combined DFT and EXAFS study. Geochimica *et Cosmochimica Acta,* vol. 73, 5975 - 5988.

HEINE, T.; RAPACIOLI, M.; PATCHKOVSKII, S.; FRENZEL, J.; KOESTER, A. M.; CALAMINICI, P.; ESCALANTE, S.; DUARTE, H. A.; FLORES, R.; GEUDTNER, G.; GOURSOT, A.; REVELES,J. U.; VELA, A.; SALAHUB, D. R - http://www.demon-software.com/public_html/index.html. Accessed: August, 08th 2010.

HERING J. G., CHEN P. Y., WILKIE J. A. and ELIMELECH M. (1997). Arsenic removal from drinking water during coagulation. *Journal of Environmental Engineering,* vol. 123, 800 - 807.

KUBICKI, J . D.; KWON, K.; D. PAUL, K. W. and SPARKS, D. L. (2007). Surface complex structures modeled with quantum chemical calculations: carbonate, phosphate, sulphate, arsenate and arsenite. European Journal of Soil Science, vol. 58, p. 932–944.

KUBICKI J.D. (2005). Comparison of As (III) and As (V) complexation onto Al and Fe-hydroxides. *In: Advances in Arsenic Research: Integration of Experimental and Observational Studies and Implications for Mitigation*. Eds P. O'Day, D. Vlassopoulos and L. Benning, ACS Symposium Series, vol. 915, 104 - 117, Washington DC.

KYLE J. H., POSNER A. M. and QUIRK J. P. (1975). Kinetics of isotopic exchange of phosphate adsorbed on gibbsite. *Journal of Soil Science,* vol. 26, 34 - 43.

LADEIRA A. C. Q. and CIMINELLI V. S. T. (2004). Adsorption and desorption of arsenic on an oxisol and its constituents. *Water Research,* vol. 38, 2087 - 2094.

LADEIRA A. C. Q., CIMINELLI V. S. T., DUARTE H. A., ALVES M. C. M. and RAMOS A. Y. (2001). Mechanism of anion retention from EXAFS and density functional calculations: Arsenic (V) adsorbed on gibbsite. *Geochimica et Cosmochimica Acta,* vol. 65, 1211 - 1217.

MACEDO J., and BRYANT R. B. (1987). Morphology, mineralogy, and genesis of a hydrosequence of oxisols in Brazil. *Soil Science Society of America Journal* **51**, 690 - 698.

MANNING B.A., FENDORF M. and GOLDBERG S. (1998). Surface structures and stability of arsenic(III) on goethite: spectroscopic evidence for inner-sphere complexes. *Environmental Science and Technology,* vol. 32, 2383 - 2388.

MASUE Y., LOEPPERT R. H. and KRAMER T. A. (2007). Arsenate and arsenite adsorption and desorption behavior on coprecipitated aluminum:iron hydroxides. *Environmental Science and Technology,* vol. 41, 837 - 842.

McBRIDE M. B. and WESSELINK L. G. (1988). Chemisorption of catechol on gibbsite, boehmite, and noncrystalline alumina surfaces. *Environmental Science and Technology,* vol. 22, 703 - 708.

MELLO J.W.V., ROY W.R., TALBOTT J.L., and STUCKI J.W. (2006). Mineralogy and Arsenic Mobility in Arsenic-rich Brazilian Soil and Sediments. *Journal of Soils & Sediments,* vol. 6 (1), 9-19.

MENG X., KORFIATIS G. P., JING C. and CHRISTODOULATOS C. (2001). Redox transformations of arsenic and iron in water treatment sludge during aging and TCLP extraction. *Environmental Science and Technology,* vol. 35, 3476 - 3481.

MONKHORST H. J. and PACK J. D. (1976). Special points for Brillouin-zone integrations. *Physical Review B,* vol. 13, 5188 - 5192.

NORONHA, A. L. O.; GUIMARÃES, L. and DUARTE, H. A. (2007). Structural and Thermodynamic Analysis of the First Mononuclear Aqueous Aluminum Citrate Complex Using DFT Calculations. *Journal of Chemical Theory Computational* vol. 3 (3), 930 - 937.

OLIVEIRA A. F., LADEIRA A. C. Q., CIMINELLI V. S. T., HEINE T. and DUARTE H. A. (2006). Structural model of arsenic(III) adsorbed on gibbsite based on DFT calculations. *Journal of Molecular Structure: THEOCHEM,* vol. 762, 17 - 23.

OLIVEIRA A. F., SEIFERT G., HEINE T. and DUARTE H. A. (2009). Density-Functional Based Tight-Binding: an approximate DFT method. *Journal of the Brazilian Chemical Society,* vol. 20, 1193 - 1205.

PACK J. D. and MONKHORST H. J. (1977). Special points for Brillouin-zone integrations - reply. *Physical Review B,* vol. 16, 1748 - 1749.

PAKTUNC D., DUTRIZAC J., and GERTSMAN V. (2008). Synthesis and phase transformations involving scorodite, ferric arsenate and arsenical ferrihydrite: Implications for arsenic mobility. *Geochimica et Cosmochimica Acta* vol. 72, 2649 – 2672

PANTUZZO F. L., and CIMINELLI V. S. T. (2010). Arsenic association and stability in long-term disposed arsenic residues. *Water Research,* vol.44, 5631 - 5640

RAVEL B. and NEWVILLE M. (2005). Athena, Artemis, Hephaestus: data analysis for X-ray absorption spectroscopy using IFEFFIT. *Journal of Synchrotron Radiation,* vol. 12, 537 - 541.

RODRIGUES, G. S.; CUNHA, I. S.; SILVA, G. G.; NORONHA, A. L. O.; ABREU, H. A.;and DUARTE, H. A. (2010). DFT Study of Vanadyl (IV) Complexes with low molecular mass ligands: picolinate, oxalate, malonate, and maltolate. *International Journal of Quantum Chemistry vol.* 111, 1395–1402.

SAALFELD H. and WEDDE M. (1974). Refinement of crystal-structure of gibbsite, $Al(OH)_3$. *Zeitschrift für Kristallographie,* vol. 139, 129-135.

SCHAEFER C. E. G. R., FABRIS J. D and. KER J. C. (2008). Minerals in the clay fraction of Brazilian Latosols (Oxisols): a review. *Clay Minerals,* vol. *43*, 137 – 154.

SHERMAN, D. and RANDALL, S. R. (2003). Surface complexation of arsenic(V) to iron(III) (hydr)oxides: Structural mechanism from ab initio molecular geometries and EXAFS spectroscopy. *Geochimica et Cosmochimica Acta*, vol. 67 (22), 4223 - 4230.

SILVA, J; MELLO, J. W.V; GASPARON, M., ABRAHÃO, W. A.P. and JONG, T. (2007). Arsenate adsorption onto aluminium and iron (hydr)oxides as an alternative for water treatment In: IMWA Symposium 2007: Water in Mining Environments, Eds: R. Cidu and F. Frau, Cagliari, Italy.

SILVA J, MELLO J. W. V, GASPARON M., ABRAHÃO W. A. P., CIMINELLI V. S. T, and JONG T. (2010). The role of Al-Goethites on arsenate mobility. *Water Research,* vol. 44, 5684 – 5692.

VASCONCELOS I. F., HAACK E. A., MAURICE, P. A. and BUNKER B. A. (2008). EXAFS analysis of Cd(II) adsorption to kaolinite. *Chemical Geology,* vol. 249, 237-249.

VOEGELIN A., KAEGI R., FROMMER J., VANTELON, and HUG D. S. J. (2010). Effect of phosphate, silicate, and Ca on Fe(III)-precipitates formed in aerated Fe(II)- and As(III)-containing water studied by X-ray absorption spectroscopy. *Geochimica et Cosmochimica Acta* vol. 74 164 - 186.

WEERASOORIYA R., TOBSCHALL H. J., WIJESEKARA H. K. D. K. and BANDARA A. (2004). Macroscopic and vibration spectroscopic evidence for specific bonding of arsenate on gibbsite. *Chemosphere,* vol. 55, 1259 - 1270.

WEERASOORIYA R., TOBSCHALL H. J., WIJESEKARA H. K. D. K., ARACHCHIGE E. K. I. A. K. U. K. and PATHIRATHNE K. A. S. (2003). On the mechanistic modeling of As(III) adsorption on gibbsite. *Chemosphere,* vol. 51, 1001 - 1013.